Studies on molecular mechanisms of the cell surface exposure of phosphatidylserine in interferon-γ-induced necroptosis

Jiancheng Chen

Contents

Abstract

In apoptotic cells, just before execution of cell death, phosphatidylserine (PS), an anionic phospholipid enriched in the inner leaflet of the plasma membrane, is exposed from the inner leaflet to the outer leaflet, and serves as an "eat me" signal to promote phagocytosis by macrophages. Interestingly, PS was recently found to be exposed prior to cell death during tumor necrosis factor (TNF)-induced necroptosis in the absence of caspase-8 activity. In this study, I demonstrated that interferon (IFN)-γ also induced PS exposure and necroptosis in *Caspase-8*-knockout mouse embryonic fibroblasts (C8KO MEFs), in accord with that in wild-type MEFs co-treated with the pan-caspase inhibitor, z-VAD-fmk. IFN-γ-induced PS exposure was significantly detected after 6 h treatment with IFN-γ, prior to the induction of necroptotic cell death observed after 24 h. To clarify the underlying molecular mechanisms of IFN-γ-induced PS exposure, we generated C8KO MEF-derived cell lines without expression or with a trace expression of RIPK3, a critical molecule in TNF-induced necroptosis. As expected, IFN-γ-induced PS exposure and necroptotic cell death were shown to be inhibited by the loss of RIPK3; however, they were restored by the exogenously expressed RIPK3. Furthermore, down-regulated expression of MLKL, a key factor for inducing membrane rupture downstream of RIPK3 in necroptosis, completely abrogated the IFN-γ-induced PS exposure and necroptosis in C8KO MEFs. Importantly, PS-exposing bubbles were formed around the cells after 6 h IFN-γ treatment, and shed from the cell surface after 24 h, similar to recently reported vesicle trafficking in TNF-induced necroptosis, implying that IFN-γ-induced formation and shedding of the PS-exposing bubbles may share the same mechanisms as those of TNF-induced necroptosis. On the other hand, in human colorectal adenocarcinoma derived HT29 cells, results showed that not only PS exposure but also necroptosis was similarly induced by IFN-γ treatment in the presence of Smac mimetics and z-VAD-fmk. The removal of IFN-γ from 6 h IFN-γ-treated PS-exposing MEFs completely inhibited necroptotic cell death, but not the subsequent increase in the number of PS-exposing cells. Taken together, PS exposure

mediated by RIPK3-activated MLKL oligomers was induced by a treatment with IFN-γ for a significant interval of time before the induction of necroptotic cell death.

Chapter 1

Introduction

1.1 Phosphatidylserine and scramblase

Phospholipids are well known to be heterogeneously distributed between the inner and outer leaflets of the plasma membrane. Among the phospholipids, phosphatidylserine (PS) is the most abundant negatively charged molecule in eukaryotic membranes and preferentially distributes in the inner leaflet of the plasma membrane (1). PS is well known to be exposed from the inner to the outer leaflet of the plasma membrane during apoptosis (2), and the cell surface PS serves as an "eat me" signal to promote phagocytosis (3, 4). Scramblase is a protein responsible for the translocation of phospholipids between the inner and outer leaflets of the cell membrane; it non-specifically and bidirectionally transports phospholipids in an ATP-independent manner (5). Remarkably, Xkr8, the caspase-dependent protein with a cleavage site of caspase-3 for its function, has been recently identified as the scramblase responsible for promoting PS exposure during apoptosis (6, 7, 8). Furthermore, substantial evidence indicates that TMEM16F, a calcium-dependent but caspase-independent transmembrane protein is another phospholipid scramblase in the plasma membrane and linked to coagulation reactions (9). In contrast to apoptosis, PS exposure was previously considered not to be induced during execution of necrosis, which was defined as a passive cell death (10).

1.2 Clearance of apoptotic cells through phagocytosis by macrophages

Apoptosis, or programmed cell death, is defined by a set of morphological changes that is induced in cells as they die (11), including cell shrinkage, chromatin condensation, and blebbing of plasma membranes. Apoptosis is an evolutionarily conserved cell death process that removes unwanted or harmful cells. Every day, numerous damaged or senescent cells undergo apoptosis, and apoptotic cells are rapidly engulfed by macrophages before they undergo rupture (3, 12). The apoptotic cell death and prompt clearance of apoptotic cells by phagocytes are very important processes for normal development and maintaining tissue homeostasis (13). During the clearance process, recognition and engulfment of apoptotic cells are two critical events (14). For

recognition of apoptotic cells, the cells must display an “eat me” signal, which is the PS exposure. Then, the milk fat globule epidermal growth factor 8 (MFG-E8), a glycoprotein which is secreted by activated macrophages and immature dendritic cells, specifically binds to PS via its factor VIII-homologous domain. In order to execute engulfment of the apoptotic cells, the PS-bound MFG-E8 needs to bind to the integrin on the surface of macrophages via an RGD motif in its EGF domain (15), and then engulfment of apoptotic cells is performed by macrophages through phagocytosis (Fig. 1). Therefore, MFG-E8 acts as a bridging molecule between apoptotic cells and phagocytes to induce phagocytosis of apoptotic cells.

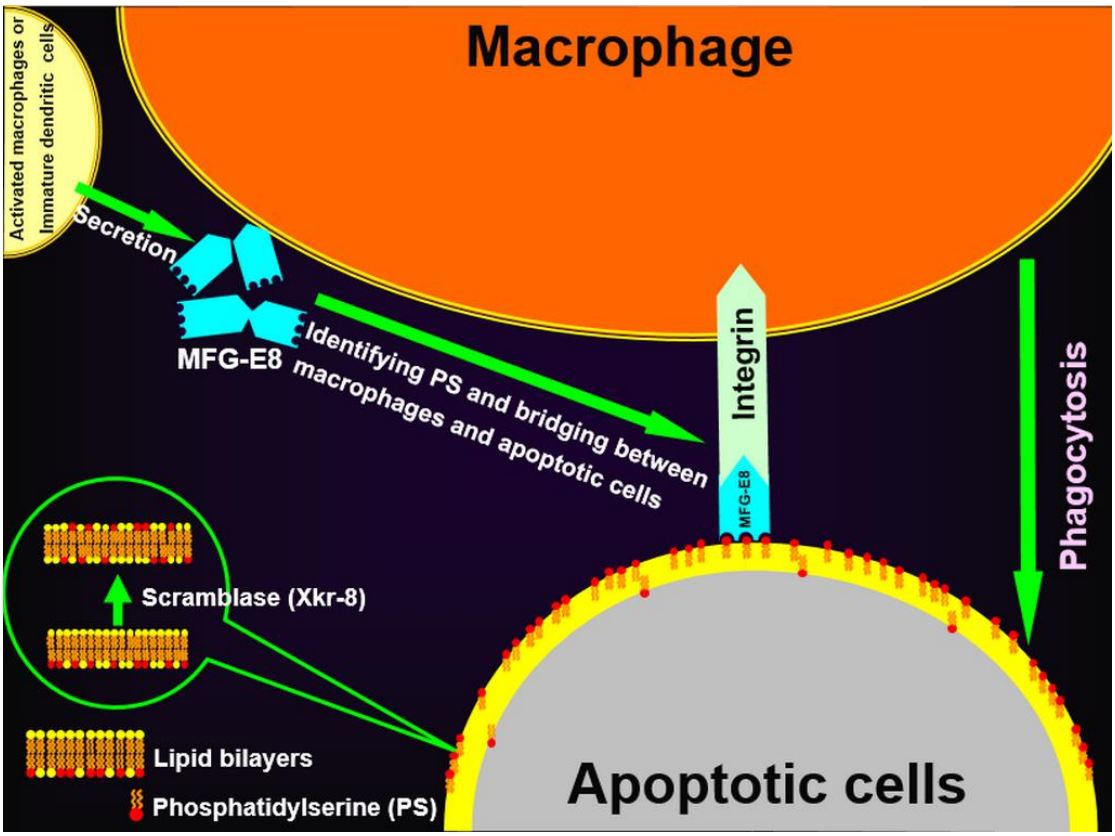

Figure 1. Schematic diagram for engulfment of PS-exposing apoptotic cells via MFG-E8. PS is an anionic phospholipid which is localized in the inner leaflet of the plasma membrane. It is exposed from inner leaflet to outer leaflet during apoptosis. And PS is exposed prior to induction of apoptotic cell death through activation of a scramblase, Xkr8. Macrophages recognize PS by utilizing a secreted glycoprotein, MFG-E8 which is secreted by activated macrophages and immature dendritic cells. MFG-E8 specifically binds to PS and mediates the engulfment of apoptotic cells by macrophages. These PS-exposing apoptotic cells are rapidly removed by macrophages through phagocytosis.

1.3 Necroptosis and its critical molecules, RIPK3 and MLKL

Necroptosis is a non-apoptotic regulated form of necrosis which is suppressed by caspase-8 (16, 17), and morphologically characterized by cell rounding, cell volume increase, organelle swelling, and the bursting of the cytoplasmic membrane (18, 19). Similar to apoptosis induced by the extrinsic pathway (20), necroptosis is triggered by the binding of various inducers, including tumor necrosis factor (TNF), Fas ligand, TNF-related apoptosis-inducing ligand (TRAIL) and certain pathogens, to their receptors, including TNF receptor 1, Fas, TRAIL receptors and Toll-like receptors, respectively (17). Among them, the most characterized system is TNF-induced necroptosis. The signaling pathway required for TNF-induced necroptosis proceeds by the protein kinase function of receptor-interacting protein kinase 1 (RIPK1) and its related kinase, RIPK3 (21). RIPK3 is phosphorylated and activated by associating with RIPK1 via a RIP homotypic interacting motif (RHIM). The activation of RIPK3 is negatively regulated by caspase-8 together with FADD and a caspase-like molecule, c-$FLIP_L$ (22, 23), and association of RIPK3 with RIPK1 is negatively regulated by the ubiquitin ligases cIAP1 and cIAP2 (24) which poly-ubiquitinate RIPK1 to arrest the integration of RIPK1 into the signaling protein complex with RIPK3. In the absence of caspase-8 activity, necroptosis can be induced by TNF-α, and activated RIPK3 mediates a necroptosis-inducing signal by activating a pseudokinase, mixed lineage kinase domain-like protein (MLKL) (25, 26). MLKL binds to RIPK3 through its kinase-like domain to form a necrosis-inducing signaling complex, termed necrosome, and is activated by phosphorylation by RIPK3. After the phosphorylation of MLKL, a conformational change unleashes the four-helix bundle domain in MLKL (27, 28), which allows activated MLKL to oligomerize and translocate to the plasma membrane; then membrane disruption and subsequent cell death are eventually induced by the oligomerized MLKL (26) (Fig. 2). The necroptotic process requires the inhibition of caspase-8 activity, which can be achieved by utilizing genetical or pharmacological methods (23, 29). Recent studies showed that PS exposure was induced during TNF-induced necroptosis, and PS-exposing cells were shown to rapidly die by necroptosis

(30, 31).

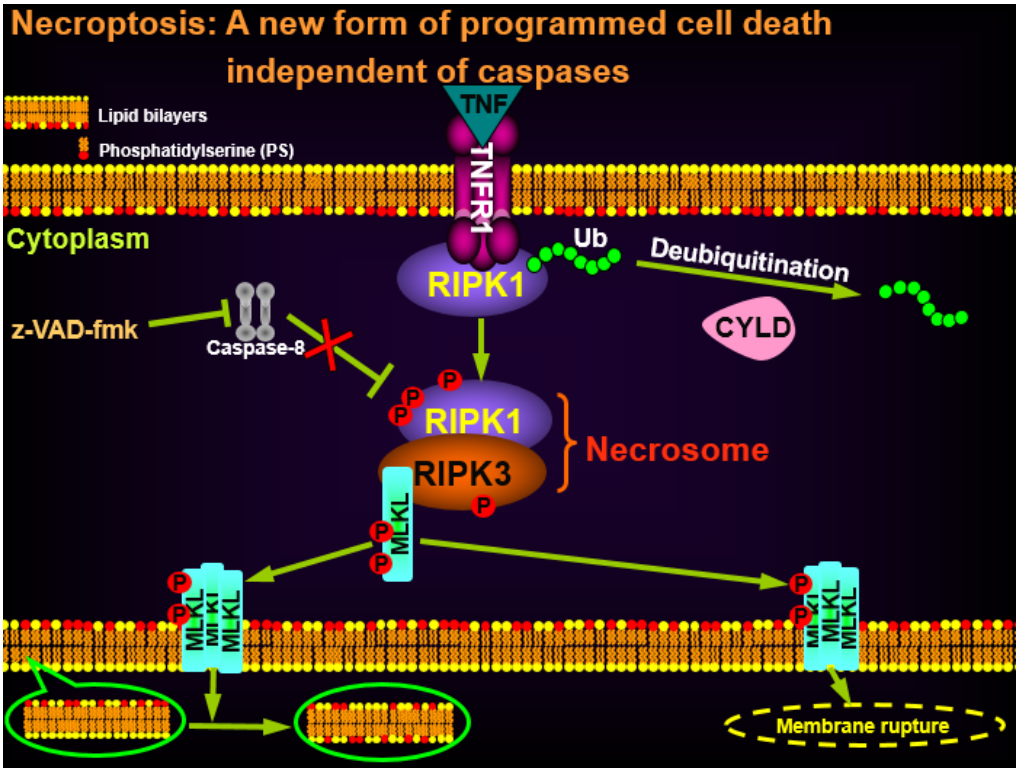

Figure 2. Necroptosis is a new form of programmed cell death, independent of caspases. In the absence of caspase-8 activity, once TNFR1 is activated by TNF, RIPK1 is deubiquitinated by CYLD, disassociates from TNFR1, and then binds to RIPK3 to form a protein complex, termed necrosome. In the necrosome, RIPK3 is phosphorylated by RIPK1, and the activated RIPK3 recruits MLKL into the necrosome and phosphorylates MLKL. The activated MLKL oligomerizes and translocates to the plasma membrane, and finally induces membrane rupture and subsequent cell death. Importantly, PS exposure is recently reported to be induced prior to the induction of cell death during TNF-induced necroptosis.

1.4 Interferons

Interferons (IFNs), which are classified into two groups, type-I (IFN-α/β) and type-II (IFN-γ) (32), and play crucial roles in mediating antiviral and anti-cell growth responses, and in modulating immune responses. Both types of IFN activate quite similar, but distinct JAK-/STAT-dependent signaling cascades downstream of their receptors to induce the expression of hundreds of specific genes (33), which collaboratively mediate many biological activities, including cytotoxic and antiproliferative effects (34, 35). However, the collaboration mechanism of genes in these processes is still not completely clear, and how the IFNs induce cell death is less

well known. On the other hand, IFN-α is well known as an antiviral and antitumor biotherapeutic agent and was exploited for clinical usage for several decades. Since IFN-γ, the only type II IFN, exerts lots of similar biological effects to IFN-α, many clinical trials with recombinant IFN-γ were carried out to determine its potential against a variety of cancers and other diseases.

In this study, I demonstrated that the IFN-γ induced necroptosis when the activity of caspase-8 was inhibited. Importantly, similar to apoptosis, I found that PS was exposed on the outer plasma membrane for a considerable time (at least 10 h) prior to the induction of necroptotic cell death. Using mouse embryonic fibroblasts, I confirmed that activations of RIPK3 and MLKL are critical for IFN-γ-induced PS exposure. My results strongly indicated that oligomerized MLKL translocated to plasma membrane would contribute to externalization of PS to the outer leaflet of the plasma membrane. Collectively, these findings provide a novel molecular mechanism for PS exposure in IFN-γ-induced necroptosis, and I propose a new potential function of MLKL to indirectly (or possibly directly) externalize PS on the plasma membrane without disrupting membrane integrity.

Chapter 2

Materials and methods

2.1 Cell lines

Primary wild type (WT) and caspase-8 knockout (C8KO) mouse embryonic fibroblasts (MEFs) with Balb/c or C57BL/6 genetical backgrounds (36, 37) were generated in this laboratory. TMEM16F KO MEFs (9) were kindly provided by S. Nagata (Osaka University). Immortalized MEF lines were generated by repeating cell passage for at least one month. These MEFs, human colorectal adenocarcinoma-derived HT29 cells, and human embryonic kidney-derived 293T cells were cultured in Dulbecco's modified Eagle's medium (DMEM, Nacalai Tesque) supplemented with 10% fetal bovine serum (FBS, BioWest), 100 units/ml penicillin, and 100 μg/ml streptomycin (Nacalai Tesque). Chinese hamster ovary (CHO) cells were cultured in a mixture of DMEM and Ham's 12 medium (Nissui) (ratio is 1:1) supplemented with 5% FBS, 50 units/ml penicillin, and 50 μg/ml streptomycin.

2.2 Reagents

The reagents used in experiments are shown as below.

Table 1: The reagents used in experiments.

Reagent name	Abbreviation	Function	Maker
z-VAD-fmk	Z	pan-caspase inhibitor	Peptide Institute
mouse and human IFN-γ	I	necroptosis inducer	Pepro Tech
mouse TNF-α	T	necroptosis inducer	ProSpec
Staurosporine	STS	apoptosis inducer	Alomone Labs
Necrostatin-1	N	RIPK1 inhibitor	Santa Cruz Biotechnology
anti-mouse TNF-α antibody	(none)	TNF-α inhibitor	Biolegend
Smac mimetics	S	IAP inhibitor	AdooQ Bioscience
necrosulfonamide	NSA	human MLKL inhibitor	Toronto Research Chemicals
cycloheximide	C	protein synthesis inhibitor	Nacalai Tesque
propidium iodide	PI	dead cells indicator	Nacalai tesque
Polyethyleneimine "Max"	PEI	Transfection reagent	Polysciences

2.3 Vectors and plasmids for lentiviral infection

Lentiviral vectors, pCAG-HIVgp (packaging plasmid) and pCMV-VSV-G-RSV-Rev (an expression vector of the vesicular stomatitis virus G glycoprotein and HIV Rev) were kindly provided by H. Miyoshi (RIKEN, Japan), and other expression vectors

were prepared as described previously (38). The main expression vectors used in my experiments are briefly described below.

For expression of mouse RIPK3, its cDNA (GenBank accession number NM_019955.2) was subcloned and inserted into a lentiviral expression vector, pCSII-PGK-3xFlag-MCS-IRES-puro. To prepare the RHIM domain mutant of RIPK3, the amino acid sequence, ^{422}GTPWYPWTPPNPMTGPPALVFNNCSE**VQIG**NYNSLVAPPR^{461} in the RHIM domain of mouse RIPK3 was replaced with ^{422}GTPWYPWTPPNPMTGPPALVFNNCSE**AAAA**NYNSLVAPPR^{461}.

For expression of GFP-conjugated milk fat globule-EGF factor 8 (MFG-E8-GFP) (39), the original plasmid, pEF-BOS-MFG-E8 (D89E) (14, 15), was kindly provided by S. Nagata (Osaka University, Japan). C-terminal GFP-fused MFG-E8 cDNA was subcloned from this original plasmid and inserted into a lentiviral expression vector, pCSII-EF-MCS-IRES-puro. All the generated constructs shown above were verified by DNA sequencing (Applied Biosystems).

The lentiviral infection procedure is simply described as follow. Under protection level 2 (P2) environment, 293T cells were cultured until ~70% confluency on one 10 cm dish, and then co-transfected with a designated expression vector, pCAG-HIVgp and pCMV-VSV-G-RSV-Rev (ratio is 11.2 μg: 6.4 μg: 6.4 μg) using PEI transfection reagent (40-42) (total amount of DNA: PEI=24 μg: 192~384 μl. A detailed protocol was referred to the manufacturer's instructions of Lipofectamine 2000 (Invitrogen)). Cultured supernatants containing virus particles were collected at 36 hours post-transfection, filtered with a 0.45 mm filter (Millipore), and concentrated by centrifuging at 6,000 rpm for ~16 hours at 4 ^{o}C. The concentrated virus-containing supernatants were then added to cells and cultured for at least 24 hours for infection. Infected cells were cultured through passage for at least 3 times under P2 environment. Then, cells were transferred to a P1 environment for cell culture and analyses.

2.4 Preparation of MFG-E8-GFP solution

To detect PS-exposing cells, MFG-E8-GFP was prepared and used to stain cells. To prepare the MFG-E8-GFP-containing solution, pCSII-EF-MFG-E8-GFP-IRES-puro was introduced into CHO cells by lentiviral infection. After 2 μg/ml puromycin (InvivoGen) selection for 2 days, highly MFG-E8-GFP-expressing CHO cells were sorted by a FACSAria III system (BD Biosciences). The sorted cells were cultured until 80% confluency, washed with PBS twice, and cultured with ASF104 medium (AJINOMOTO) supplemented with 1% FBS (BioWest) at 37 ^{o}C in a 5% v/v CO_2 humidified incubator for 2 days to produce MFG-E8-GFP protein. The cultured ASF104 medium supernatant was then collected, filtered through a 0.45 μm filter (Millipore), and used as the MFG-E8-GFP-containing solution, which can be directly added to cells for staining.

2.5 Gene knockdown by the shRNA expression system

To achieve the specific knockdown of mouse genes, the short hairpin RNA (shRNA) expression system with lentivirus-based vectors was utilized as previously described (43, 44). The DNA oligonucleotide sequences encoding shRNA for *Ripk3*, *Tmem16F*, and *Mlkl* are shown in Table 2.

Table 2: DNA oligonucleotide sequences of designed shRNAs.

Gene name	GenBank™ accession number	shRNA abbreviation	Sequence
Ripk3	NM_019955.2	shRipk3	5’-TATGGTTATTCTTCGTAATGA-3’
Tmem16F	NM_175344.4	sh16F	5’-GAGAATCAACATGATTAATCA-3’
Mlkl	NM_029005.2	shMlkl#1	5’-TCCCAACATCTTGCGTATATT-3’
		shMlkl#2	5’-AGATCCAGTTCAACGATATAT-3’
lacZ	V00296.1	shLacZ	5’-AAGGCCAGACGCGAATTAT-3’

2.6 Western Blotting and antibodies

The cultured cells were suspended in ice-cold lysis buffer (20 mM Tris-HCl, pH7.4, 10% glycerol, 1% Triton X-100, 0.5% Nonidet P-40, 150 mM NaCl, and 1 mM EDTA) supplemented with a protease inhibitor cocktail (Nacalai Tesque), and centrifuged at 15,000 rpm for 10 min at 4 ºC to eliminate debris. The supernatants of the cell lysates were mixed with SDS-PAGE (sodium dodecyl sulfate-polyacrylamide gel electrophoresis) sample buffer (62.5 mM Tris-HCl, 2% SDS, 10% Glycerol, 0.01% Bromophenol blue, and 0.01% Pyronin Y) containing 50 mM DTT (reducing conditions), heated at 98 ºC for 5 min, cooled on ice for 5 min, centrifuged at 15,000 rpm for 5 min at 4 ºC, resolved by 10% SDS-PAGE, transferred to PVDF membrane (Millipore), and analyzed by Western blotting as described earlier (45). Briefly, PVDF membranes were blocked in 5% skim milk-containing TBST for 1 hour at room temperature, probed with a primary antibody in 5% skim milk-containing TBST overnight at 4 ºC, washed with TBST three times (10 min/time), and then incubated with an appropriate horseradish peroxidase (HRP)-conjugated secondary antibody in TBST for 1 hour at room temperature. After washing with TBST three times (10 min/time), bands on membranes were detected by ImageQuant LAS4010 (GE Healthcare) after treatment with Immobilon Western Chemiluminescent HRP Substrate (Millipore), and quantified using MultiGauge V3.0 software (FUJIFILM).

To detect MLKL oligomers, the supernatants of cell lysates were mixed with SDS-PAGE sample buffer without DTT (non-reducing conditions), and were directly resolved by 5~15% gradient SDS-PAGE (Nacalai Tesque) and analyzed by Western blotting using anti-mouse MLKL antibody shown in Table 3.

To detect TMEM16F, the supernatants of cell lysates were mixed with SDS-PAGE sample buffer containing 50 mM DTT, and were incubated at room temperature for 30 min without heating, subjected to 5~15% gradient SDS-PAGE (Nacalai Tesque), and analyzed by Western blotting using anti-mouse TMEM16F antibody shown in Table 3.

Table 3: Primary and secondary antibodies used in Western blotting.

Primary antibody	Dilution	Cat. No/Maker	Secondary antibody	Dilution	Cat. No/Maker
anti-mouse RIPK3	1: 1000	2283/ProSci	anti-mouse IgG, HRP-linked antibody	1: 5000	7076S/Cell Signaling
anti-mouse MLKL	1: 1000	MABC604/Millipore	anti-rabbit IgG, HRP-linked antibody	1: 5000	7074S/Cell Signaling
anti-mouse phosphorylated MLKL	1: 1000	ab196436/Abcam	anti-rat IgG, HRP-linked antibody	1: 5000	7077S/Cell Signaling
anti-mouse Caspasse-3	1: 1000	611049/BD Transduction Laboratories			
anti-mouse cleaved Caspasse-3	1: 1000	9664/Cell Signaling			
anti-mouse TMEM16F	1: 5000	a kind gift from S. Nagata			
anti-actin	1: 5000	MAB1501/Millipore			

2.7 Quantitative Reverse Transcription PCR (qRT-PCR)

To detect expressions of indicated genes at the mRNA level, qRT-PCR was performed. The total RNA was isolated from cells using Sepasol RNA I Super G (Nacalai Tesque) according to the manufacturer's instructions. One μg of extracted total RNA was subjected to a reverse transcription (RT) reaction using ReverTra Ace qPCR RT Master Mix (TOYOBO). After the RT reaction, the cDNA products were diluted in Milli-Q water at a final concentration of 10 ng/μl. Then, 30 ng of the cDNA products were mixed with THUNDERBIRD SYBR qPCR Mix (TOYOBO), and real-time RT-PCR was carried out using the StepOne Real-Time PCR System (Applied Biosystems) with the primer pairs shown in Table 4. The expression levels of the mRNAs were normalized to that of *Gapdh*, and expressed as a ratio to the expression level in control cells.

Table 4: Primers for qRT-PCR.

Gene name	GenBank™ accession number	Sequence
Mlkl	NM_029005.2	Forward: 5'-GACCAAACTGAAGACAAGTA-3'
		Reverse: 5'-CTCACTATTCCAACACTTTC-3'
Tmem16F	NM_175344.4	Forward: 5'-CACGGACTTCAAGAACACAGACA-3'
		Reverse: 5'-GTCACGGTACCTGCACAAGGT-3'
Gapdh	NM_001289726.1	Forward: 5'-GATGACATCAAGAAGGTGGTGA-3'
		Reverse: 5'-TGCTGTAGCCGTATTCATTGTC-3'

2.8 Fluorescence imaging

The observation of PS exposure and cell death of IFN-γ-treated cells, and the MGF-E8-GFP$^+$ bubble formation on the PS-exposing cells were performed as described below.

MEFs were seeded into a plastic sterile 24-well culture plate (Greiner Bio-One) or a 24-well SensoPlate, PS, Glass Bottom (Greiner Bio-One), for observation of PS exposure and cell death or MGF-E8-GFP$^+$ bubbles formation, respectively. After overnight cultivation, the cells were treated with IFN-γ for indicated periods. Culture supernatants were then removed, and MFG-E8-GFP-containing solution was directly added to cells without dilution. Cells were incubated at 37 ^{o}C for 20 minutes for staining PS. Then, the cells on plastic plates with 50 ng/ml PI, and cells on glass bottom plates with 50 ng/ml PI, were analyzed under the fluorescence microscope (DMIRE2, Leica). Images of bright field, MGF-E8-GFP, and PI were taken and analyzed by MetaMorph software (Molecular Devices).

2.9 Flow cytometric analyses and cell sorting

To detect PS-exposing and dead cells after treatment with IFN-γ for the indicated periods, cells were trypsinized, resuspended in the solution containing MFG-E8-GFP and 0.2 μg/ml PI, and kept at room temperature for at least 5 minutes for staining. Cells were then directly analyzed by flow cytometry as previously described (38), using a FACSAria III system (BD Biosciences) and FACSDiva software (BD Biosciences). The

percentages of PS-exposing cells (MGF-E8-GFP^{+}PI^{-}) and dead cells (MGF-E8-GFP^{+}PI^{+}) were calculated by FlowJo software (version 7.6.5, Tree Star).

For sorting the PS-exposing cells, MEFs were treated with IFN-γ for 6 hours, trypsinized, and resuspended in the solution containing MFG-E8-GFP and 0.2 μg/ml PI. After a 5 min incubation, PS-exposing cells were gated by FACSDiva software and sorted according to the manufacturer's instructions using a FACSAria III system. Sorted PS-exposing cells were collected to be analyzed by flow cytometry to confirm the ratio of PS-exposing cells, or to be cultured for further analyses.

Chapter 3

Results

3.1 PS is exposed prior to cell death in IFN-γ induced necroptosis

It is well known that PS is exposed before cell death during apoptosis, and recently, PS was reported to be exposed similarly prior to cell death during TNF-α-induced necroptosis (31). Interestingly, we found that IFN-γ also induced necroptotic cell death in MEFs in the presence of z-VAD-fmk, a pan-caspase inhibitor which blocks protease activities of various caspases, including caspase-8, and this process took a longer interval of time (at least 18~24 h) when compared with TNF-α-induced necroptosis (about 4~6 h). Therefore, to investigate whether PS exposure is induced during this IFN-γ-induced necroptotic process, various experiments were carried out.

3.1.1 Both PS exposure and cell death are induced by IFN-γ-treatment in primary MEFs in the presence of z-VAD-fmk

In this experiment, primary WT MEFs with a Balb/c genetic background were used. I firstly confirmed that PS was exposed before the induction of cell death in TNF-α-induced necroptosis (Fig. 3A). I found that the PS exposure and cell death induction processes took a short interval of time (2 h for PS exposure and 4 h for cell death). Then, the primary WT MEFs were treated with IFN-γ and z-VAD-fmk (IZ). IZ-treated cells were stained with MGF-E8-GFP and PI, and monitored by fluorescence microscopy (Fig. 3B) and flow cytometry (Fig. 3C). The amounts of PS-exposing cells (MGF-E8-GFP^+PI^-) and dead cells (MGF-E8-GFP^+PI^+) were quantitively summarized in Fig. 3D. I found that primary WT MEFs significantly died at 24 h after IFN-γ treatment in the presence of z-VAD-fmk. On the other hand, PS-exposing cells were detectable at 6 h after IFN-γ treatment, while dead cells were hardly detected. Neither PS exposure nor cell death was found in the primary WT MEFs treated with IFN-γ only or z-VAD-fmk only (data not shown). These results indicate that cell death is induced by IFN-γ in the absence of caspase-8 activity, and PS is exposed prior to cell death for more than 10 h.

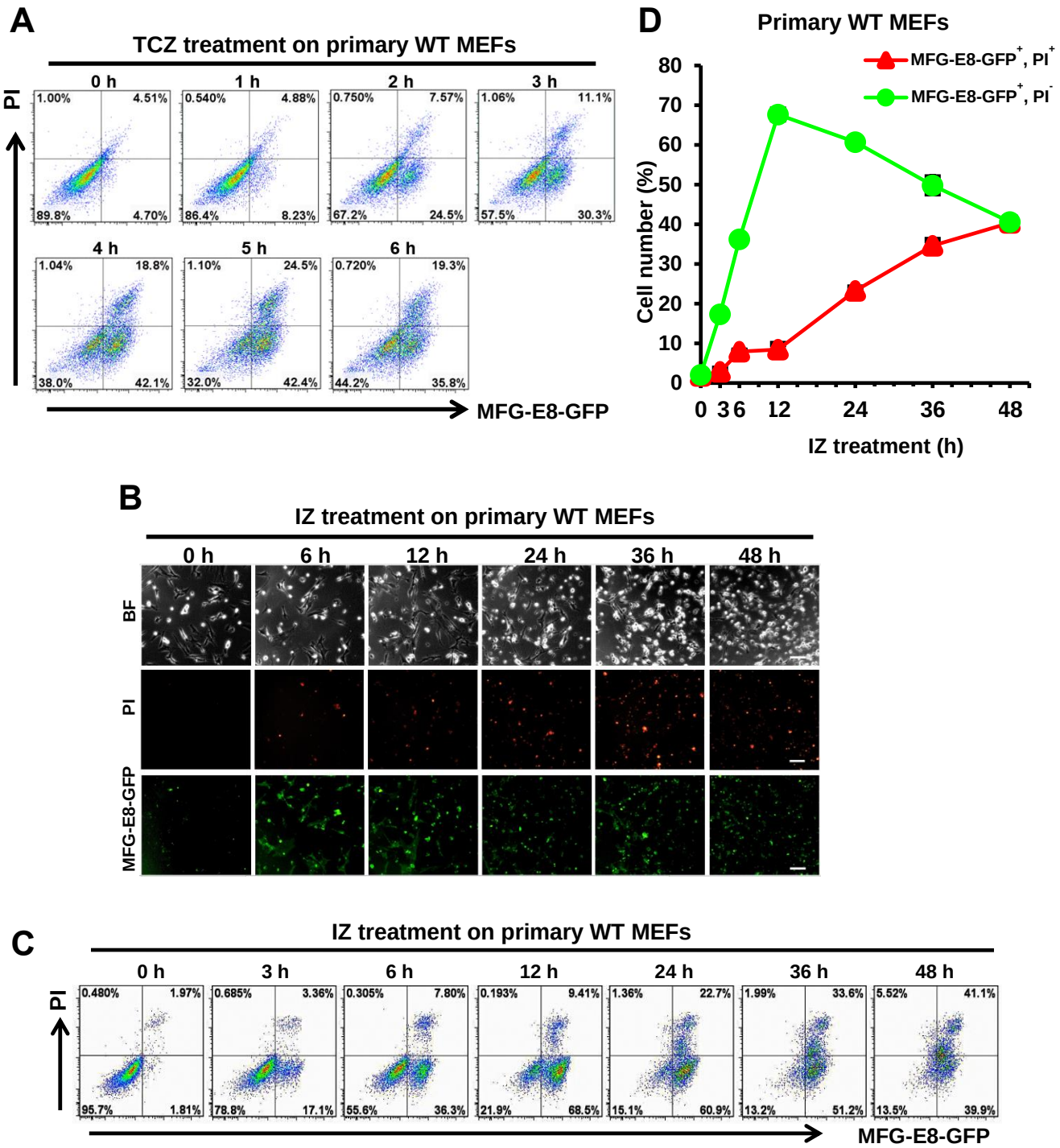

Figure 3. IFN-γ induces PS exposure in primary WT MEFs before the induction of cell death. **A**, primary WT MEFs were treated with 10 ng/ml TNF-α, 1 μg/ml cycloheximide, and 50 μM z-VAD-fmk (TCZ) for the indicated periods. Cells were stained with MFG-E8-GFP and PI to monitor PS exposure and cell death, respectively, and analyzed by flow cytometry. **B** and **C**, primary WT MEFs were treated with 10 ng/ml IFN-γ and 50 μM z-VAD-fmk (IZ) for the indicated periods. Cells were stained with MFG-E8-GFP and PI, analyzed by fluorescent microscopy (**B**) and flow cytometry (**C**). BF: bright field. **D**, the data of the flow cytometric analysis (**C**) were graphically shown. Representative flow cytometric plots and fluorescent images of more than three experiments are shown. Scale bars represent 100 μm. The quantified data of the flow cytometric analysis are presented as mean ± S.D. (n≥3).

3.1.2 IFN-γ induced cell death is necroptosis, not apoptosis

To confirm whether the cell death induced by IFN-γ treatment is necroptosis, the IZ-treated primary WT MEFs were treated together with necrostatin-1, an inhibitor of RIPK1 which plays an important role in necroptosis (46). The cell death induced at 24 h after IFN-γ treatment was inhibited by treatment with necrostatin-1 (Fig. 4, A and B). In Western blotting analysis for caspase-3 (Fig. 4C), significant bands of cleavage of caspase-3 were not found in the IZ-treated cells, but were found in apoptotic cells exposed by UV or treated with staurosporine (STS), suggesting that IZ-induced cell death was not apoptosis. Taken together, IFN-γ-induced cell death in primary WT MEFs in the presence of z-VAD-fmk was necroptosis.

3.1.3 PS exposure and cell death are also observed in primary *Caspase-8*$^{-/-}$ MEFs after IFN-γ treatment

To further examine the PS exposure in IFN-γ-induced necroptosis, previously generated primary MEFs from *Caspase-8*$^{-/-}$ (C8KO) mice with a Balb/c genetic background (36, 37) were analyzed. I found that the primary C8KO MEFs also exposed PS after treatment with IFN-γ for 6 h and began to die after 24 h (Fig. 5). These data were similar to those of the primary WT MEFs treated with IFN-γ in the presence of z-VAD-fmk (Fig. 3A). Taken together, IFN-γ generally induced PS exposure for at least 10 h without the induction of necroptosis in the absence of caspase-8 activity in MEFs.

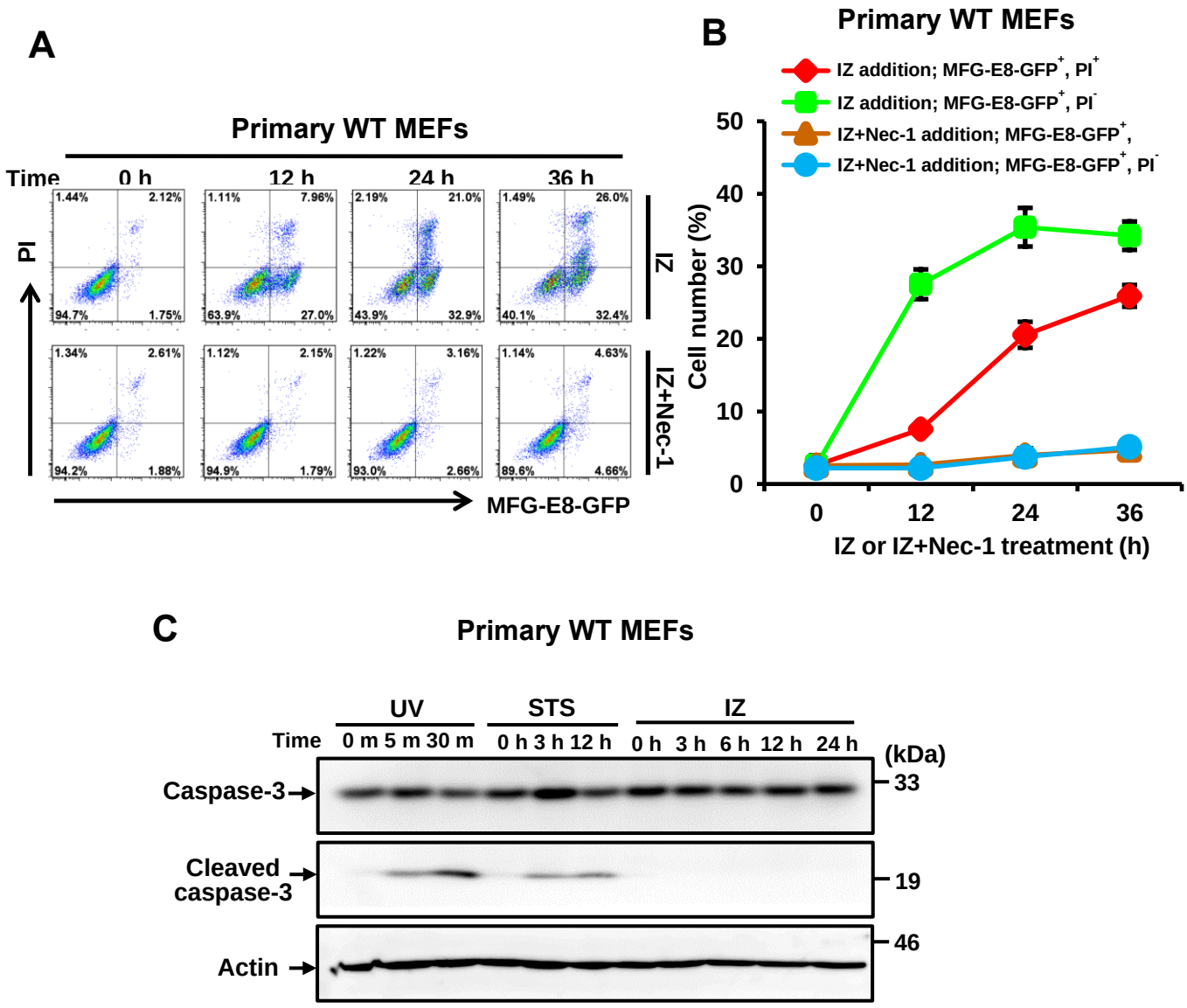

Figure 4. Necroptosis is induced by IFN-γ treatment in primary WT MEFs.
A, primary WT MEFs were incubated with or without 50 μM necrostatin-1 (Nec-1) for 30 minutes before the treatment with 10 ng/ml IFN-γ and 50 μM z-VAD-fmk (IZ) for the indicated periods. Cells were stained with MFG-E8-GFP and PI to monitor PS exposure and cell death, respectively, and analyzed by flow cytometry. **B**, the data of the flow cytometric analysis (**A**) are graphically shown. **C**, primary WT MEFs treated with 10 ng/ml IFN-γ and 50 μM z-VAD-fmk (IZ) for the indicated periods, were analyzed by Western blotting with anti-Caspase-3, anti-cleaved Caspase-3, and anti-actin antibodies. UV: Ultraviolet, intensity was 3 mW/cm^2. STS: Staurosporine, final concentration was 500 nM. Representative flow cytometric plots and Western blotting data of more than three experiments are shown. The quantified data of the flow cytometric analysis are presented as mean ± S.D. (n≥3).

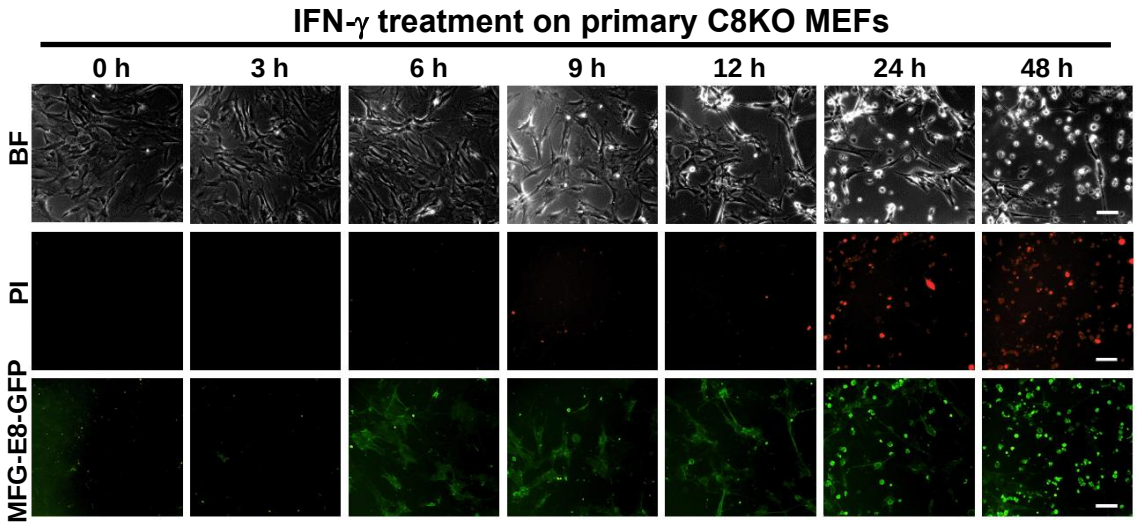

Figure 5. IFN-γ induces PS exposure in primary C8KO MEFs before the induction of necroptosis. Primary C8KO MEFs were treated with 10 ng/ml IFN-γ for the indicated periods. Cells were stained with MFG-E8-GFP and PI, and then analyzed by fluorescent microscopy. BF: bright field. Representative fluorescent images of more than three experiments are shown. Scale bars represent 100 μm.

3.1.4 Neither PS exposure nor cell death is induced by IFN-γ in immortalized C8KO MEFs

To investigate the mechanisms of IFN-γ-induced PS exposure, C8KO MEFs are necessary. However, because of the early embryonic lethality of C8KO mice, I could not obtain enough primary C8KO MEFs. Therefore, immortalized C8KO (iC8KO) MEFs with the Balb/c genetic background were generated by repeated passage for more than one month. Unexpectedly, neither PS exposure nor cell death was detected by fluorescence microscopy and flow cytometry in iC8KO MEFs (Fig. 6, A and B), suggesting that these iC8KO MEFs were resistant to IFN-γ-induced PS exposure and necroptosis.

3.2 RIPK3 plays an essential role in the PS exposure of IFN-γ-treated caspase-8 negative MEFs

3.2.1 RIPK3 is lost in iC8KO MEFs

To find out the reason why iC8KO MEFs were insensitive to IFN-γ-induced PS exposure, I examined the expression of RIPK3, an essential molecule for the induction of necroptosis. Western blotting analysis showed that RIPK3 was undetectable in iC8KO MEFs (Fig. 7), suggesting that RIPK3 expression was lost in the iC8KO MEFs.

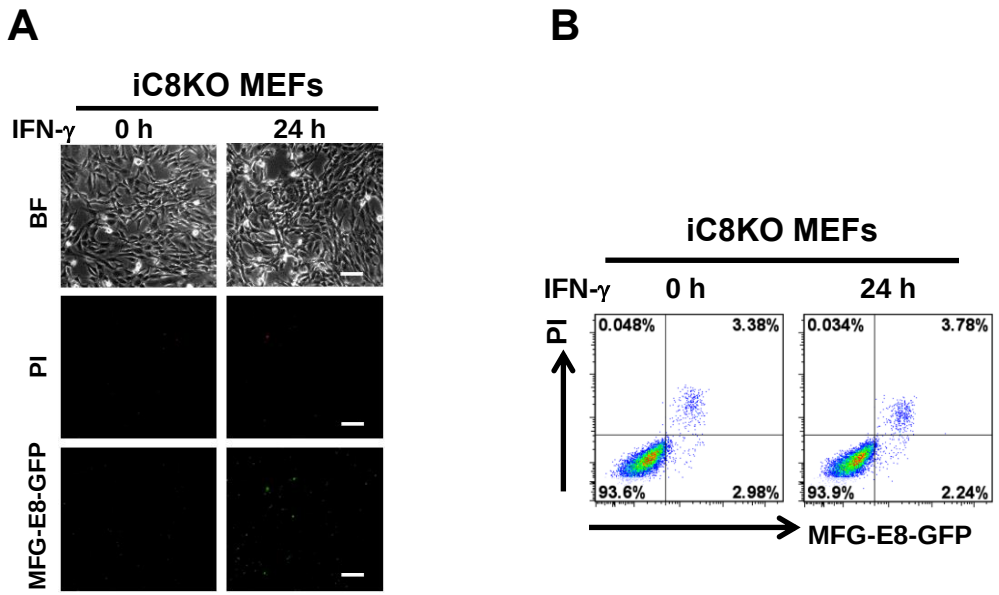

Figure 6. iC8KO MEFs are resistant to IFN-γ-induced PS exposure and cell death.
A and **B**, iC8KO MEFs were treated with 10 ng/ml IFN-γ for 24 h. Cells were stained with MFG-E8-GFP and PI, and then analyzed by fluorescent microscopy (**A**) and flow cytometry (**B**). BF: bright field. Scale bars represent 100 μm. Representative fluorescent images and flow cytometric plots of more than three experiments are shown.

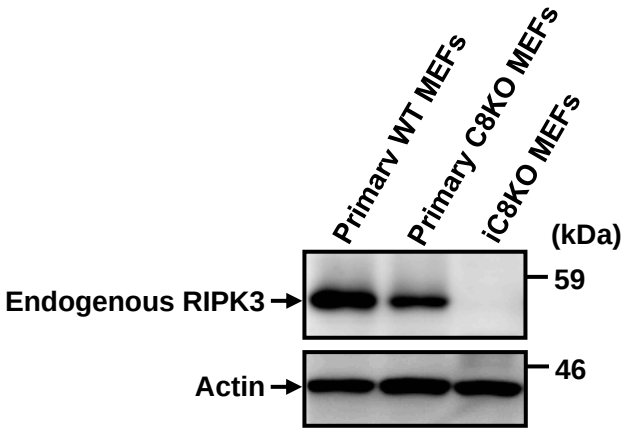

Figure 7. Expression of RIPK3 in iC8KO MEFs.
Primary WT MEFs, primary C8KO MEFs, and iC8KO MEFs were analyzed by Western blotting with anti-RIPK3 and anti-actin antibodies. Representative Western blotting data of more than three experiments are shown.

3.2.2 Exogenous expression of WT RIPK3 in iC8KO MEFs restored the PS-exposing ability after IFN-γ treatment

To clarify whether the lack of RIPK3 caused insensitivity of iC8KO MEFs to IFN-γ-induced PS exposure and necroptosis, I exogenously expressed RIPK3 in iC8KO MEFs at a similar expression level to that in primary C8KO MEFs (Fig. 8A). Then, RIPK3-expressing iC8KO (iC8KO-RIPK3) MEFs were subjected to IFN-γ treatment. I found that the iC8KO-RIPK3 MEFs began to expose PS after treatment with IFN-γ for 6 h, and the induction of cell death was observed at 24 h after IFN-γ treatment (Fig. 8, B and C). The ratio of PS-exposing cells increased in a time-dependent manner (Fig. 8D), and these results were similar to those of primary C8KO MEFs (Fig. 5), suggesting that the introduction of RIPK3 restored the PS-exposing ability in our generated iC8KO MEFs. Thus, RIPK3 is indispensable for the PS exposure in IFN-γ-induced necroptosis.

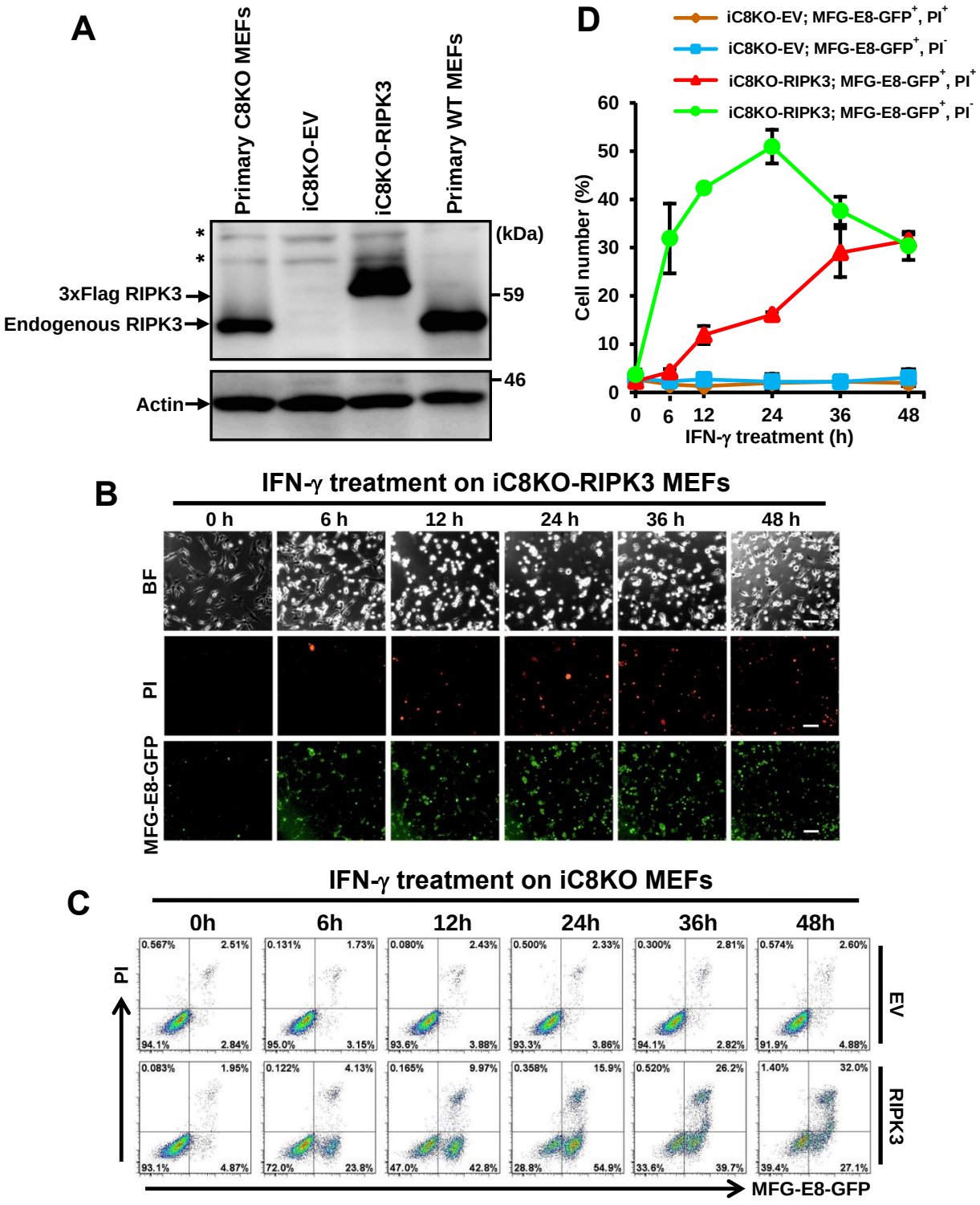

Figure 8. RIPK3 is necessary for IFN-γ-induced PS exposure in iC8KO MEFs.
A, cell lysates from primary C8KO MEFs, primary WT MEFs, and iC8KO MEFs harboring the indicated expression vectors were analyzed by Western blotting with anti-RIPK3 and anti-actin antibodies. EV: an empty vector. *: Non-specific bands. **B** and **C**, iC8KO-RIPK3 MEFs were treated with 10 ng/ml IFN-γ for the indicated periods. Cells were stained with MFG-E8-GFP and PI, and then analyzed by fluorescent microscopy (**B**) or flow cytometry (**C**). BF: bright field. Scale bars represent 100 μm. **D**, the data of the flow cytometric analysis (**C**) were graphically shown. Representative Western blotting data, fluorescent images and flow cytometric plots of more than three experiments are shown. The quantified data of the flow cytometry analysis are presented as mean ± S.D. (n≥3).

3.2.3 Autocrine TNF-α is not involved in the IFN-γ-induced PS exposure and necroptosis

I found that, similar to TNF-α-induced necroptosis, RIPK3 is also indispensable for IFN-γ-induced PS exposure and necroptosis. Then, it might be possible that IFN-γ induces TNF-α expression and the autocrine TNF-α is involved in the PS exposure and cell death after IFN-γ treatment. To exclude this possibility, I analyzed the effect of a TNF-α blocking antibody which could inhibit TNF-α-induced necroptosis, on the IFN-γ-induced PS exposure and necroptosis. Necroptotic cell death of NIH3T3 induced by TNF-α was significantly inhibited by the TNF-α blocking antibody (Fig. 9A). However, treatment with the TNF-α blocking antibody inhibited neither IFN-γ-induced PS exposure nor necroptosis in iC8KO-RIPK3 MEFs (Fig. 9B), indicating that autocrine TNF-α is not involved in the IFN-γ-induced PS exposure and cell death.

3.2.4 Introduction of RIPK3 RHIM mutant does not sensitize the iC8KO MEFs to IFN-γ

Formation of a RIPK1/RIPK3 complex is crucial for the induction of TNF-α-induced necroptosis (47), and the RIP homotypic interaction motif (RHIM) domain in RIPK1 and RIPK3 were shown to mediate their interaction (48). Therefore, the RHIM domain is necessary for induction of TNF-α-induced necroptosis (21). I then analyzed whether the RHIM domain of RIPK3 is also important for IFN-γ-induced PS exposure and necroptosis. I constructed a RIPK3 mutant in which four essential amino acid residues/VQIG of the RHIM domain were replaced by AAAA (as described in "Chapter 2 Materials and Methods"), and expressed it in the RIPK3-negative iC8KO MEFs at a similar expression level as endogenous RIPK3 in primary C8KO MEFs (Fig. 10A). After IFN-γ treatment, I found that neither PS exposure nor necroptotic cell death was induced in the iC8KO MEFs expressing the RIPK3 RHIM mutant (iC8KO-RIPK3 RHIM mutant) (Fig. 10B). This result indicated that interaction of RIPK3 and RIPK1 is also essential for IFN-γ-induced PS exposure and necroptosis.

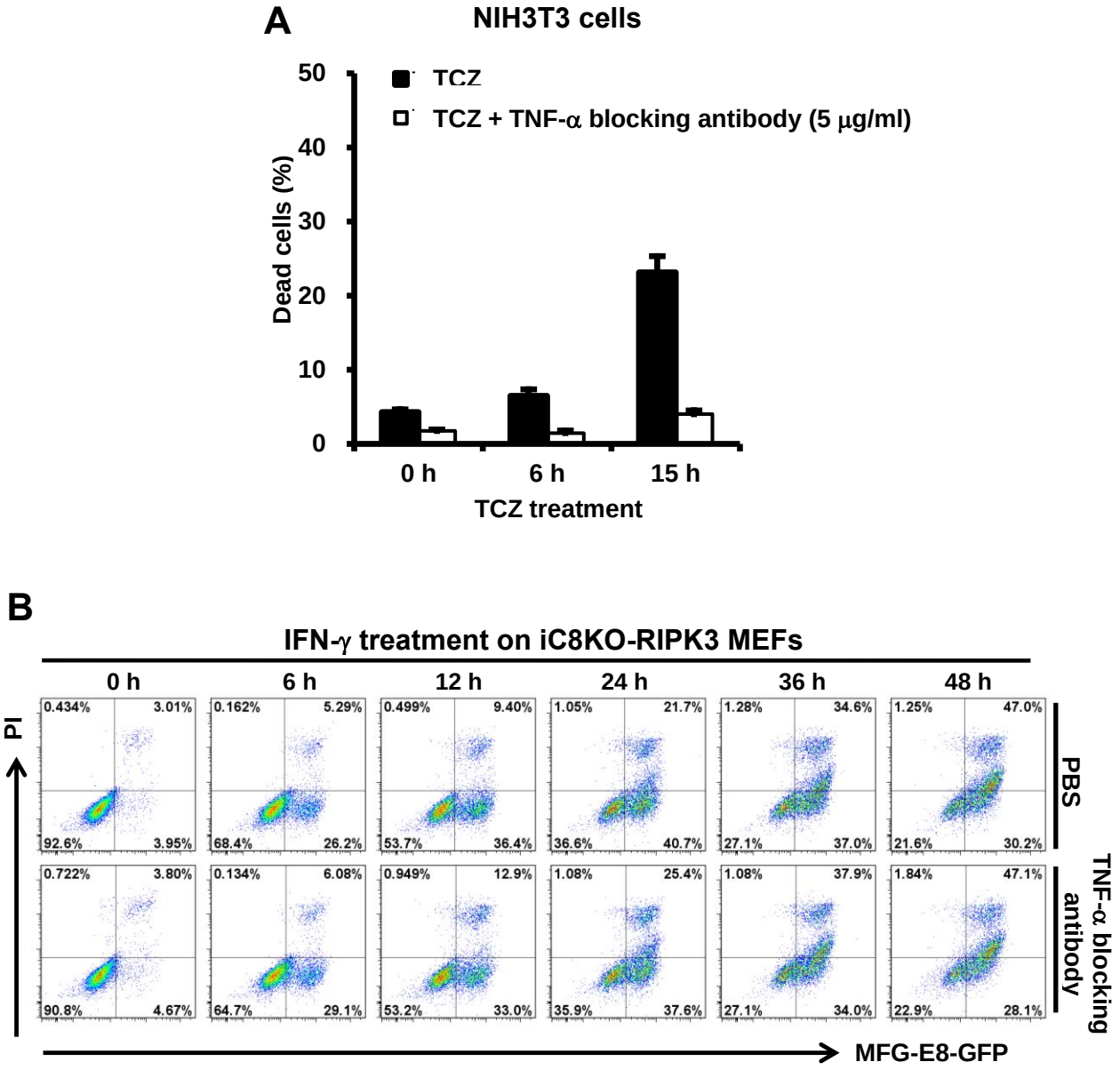

Figure 9. Effects of TNF-α blocking antibody on IFN-γ-treated iC8KO-RIPK3 MEFs. **A**, NIH3T3 cells were treated with 0.1 ng/ml TNF-α, 1 μg/ml cycloheximide, and 30 μM z-VAD-fmk (TCZ) in the presence and absence of a neutralizing antibody against TNF-α (TNF-α blocking antibody) for the indicated periods. Cells were stained with PI to monitor cell death and analyzed by flow cytometry. **B**, iC8KO-RIPK3 MEFs were treated with 10 ng/ml IFN-γ in the presence or absence of 5 μg/ml TNF-α blocking antibody for the indicated periods and analyzed by flow cytometry. Representative flow cytometric plots of more than three experiments are shown. The quantified data of cells are presented as mean ± S.D. (n≥3).

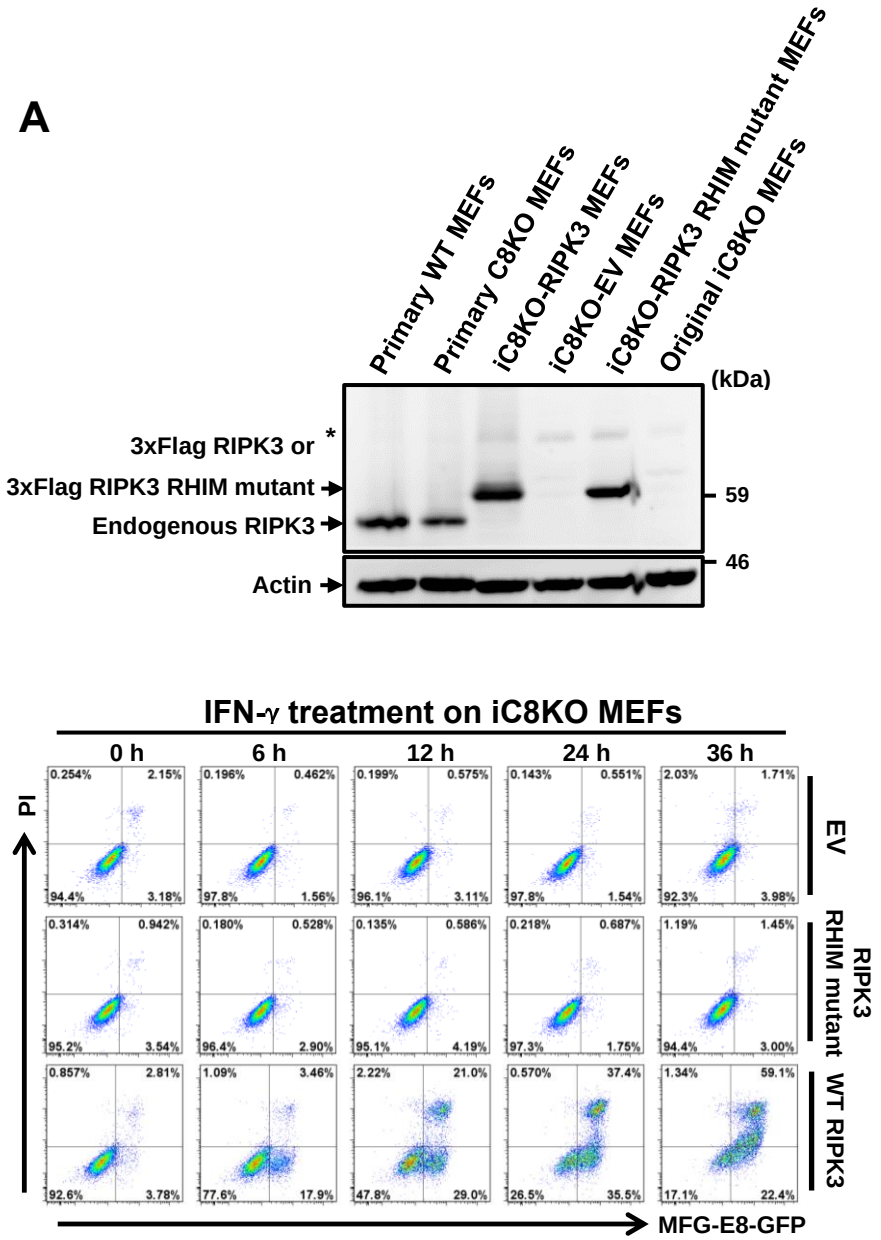

Figure 10. iC8KO MEFs expressing a RIPK3 RHIM mutant are resistant to IFN-γ-induced PS exposure and necroptotic cell death.
A, primary WT MEFs, primary C8KO MEFs, and iC8KO MEFs harboring the indicated expression vectors were analyzed by Western blotting with anti-RIPK3 and anti-actin antibodies. EV: an empty vector. *: Non-specific bands. **B**, iC8KO-EV, iC8KO-RIPK3 RHIM mutant, and iC8KO-RIPK3 MEFs were treated with 10 ng/ml IFN-γ for the indicated periods. Cells were then stained with MFG-E8-GFP and PI, and analyzed by flow cytometry. Representative Western blotting data and flow cytometric plots of more than three experiments are shown.

3.2.5 Another iC8KO MEF clone, 17e, which expresses a small amount of RIPK3 is also sensitive to IFN-γ

By repeating cell passage for more than one month, another immortalized C8KO MEF clone, termed "17e", with the C57BL/6 genetic background was generated. These 17e MEFs still expressed a small amount of RIPK3 (Fig. 11A). After 24 h IFN-γ treatment, only approximately 20% and less than 10% of 17e MEFs were shown to be PS-exposing and dead cells, respectively (Fig. 11B), indicating that 17e MEFs with low RIPK3 expression also manifested induction of PS exposure in response to IFN-γ, although the ratio of PS-exposing cells was low.

3.2.6 Overexpression or knockdown of RIPK3 in 17e MEFs enhanced or abolished IFN-γ-induced PS exposure, respectively

To further analyze the effect of the RIPK3 expression level on the IFN-γ-induced PS exposure, I then generated 17e MEFs overexpressing exogenous RIPK3 (17e-RIPK3) (Fig. 12A) and IFN-γ treatment was performed (Fig. 12B). During the period from 12 h to 36 h of IFN-γ treatment, approximately 50% and less than 10% of total 17e-RIPK3 MEFs were shown to expose PS and die, respectively. Using a shRNA specific for RIPK3, I efficiently knocked down the expression of RIPK3 in 17e MEFs (Fig. 12C) and examined the PS exposure and necroptotic cell death of the RIPK3-knockdown 17e (17e-shRipk3) MEFs after IFN-γ treatment (Fig. 12D). As expected, both PS exposure and cell death in 17e MEFs after IFN-γ treatment were completely inhibited by the knockdown of RIPK3 expression. Taken together, IFN-γ mainly induced PS exposure dependent on expression of RIPK3, but hardly induced necroptotic cell death in 17e MEFs.

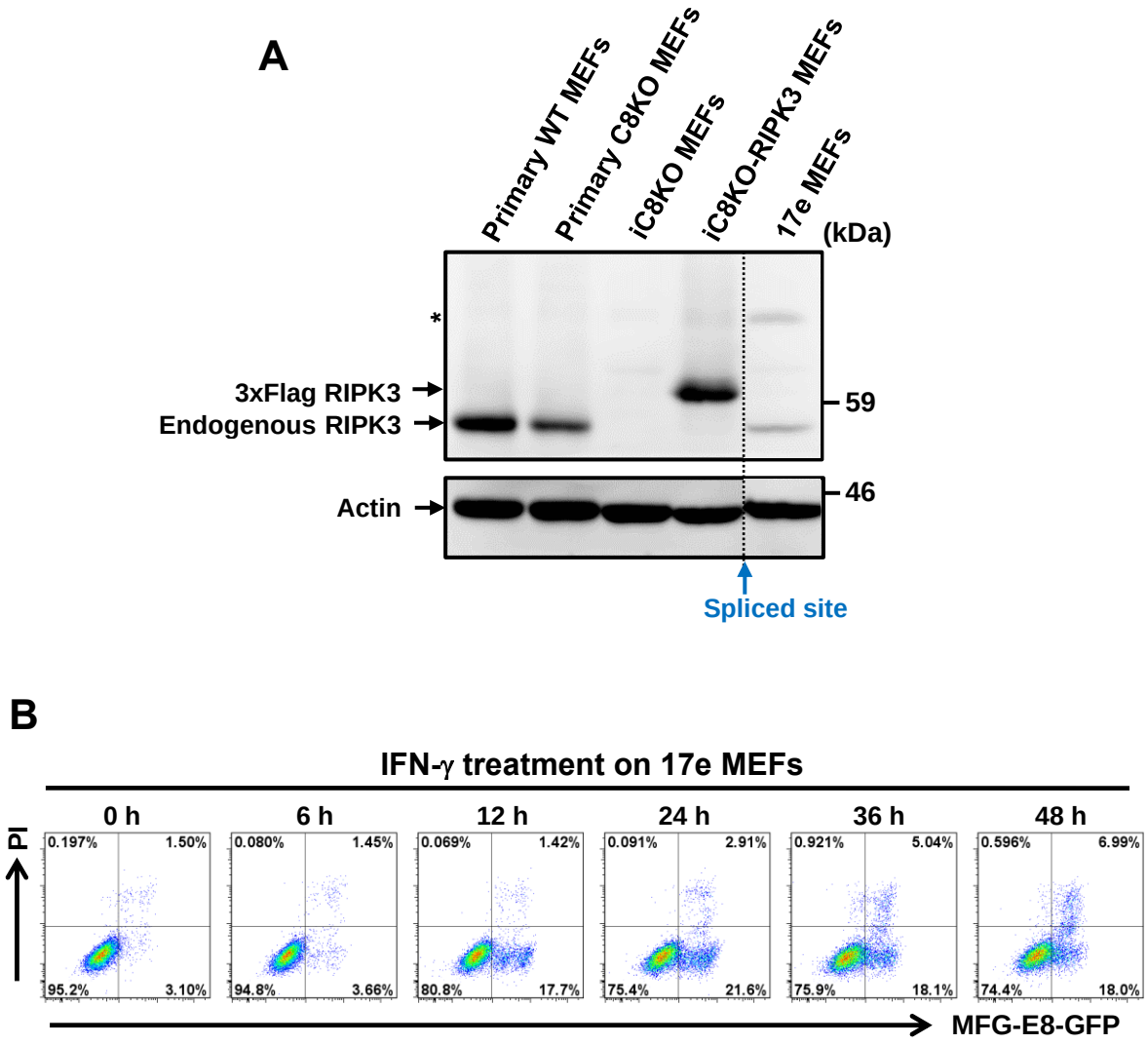

Figure 11. IFN-γ-induced PS exposure was confirmed in another iC8KO MEF clone, 17e. **A**, primary WT MEFs, primary C8KO MEFs, iC8KO MEFs, iC8KO-RIPK3 MEFs, and 17e MEFs were analyzed by Western blotting with anti-RIPK3 and anti-actin antibodies. *: Non-specific bands. Blue arrow: spliced site of two lanes from one membrane. **B**, 17e MEFs were treated with 10 ng/ml IFN-γ for the indicated periods. Cells were then stained with MFG-E8-GFP and PI, and analyzed by flow cytometry. Representative Western blotting data and flow cytometric plots of more than three experiments are shown.

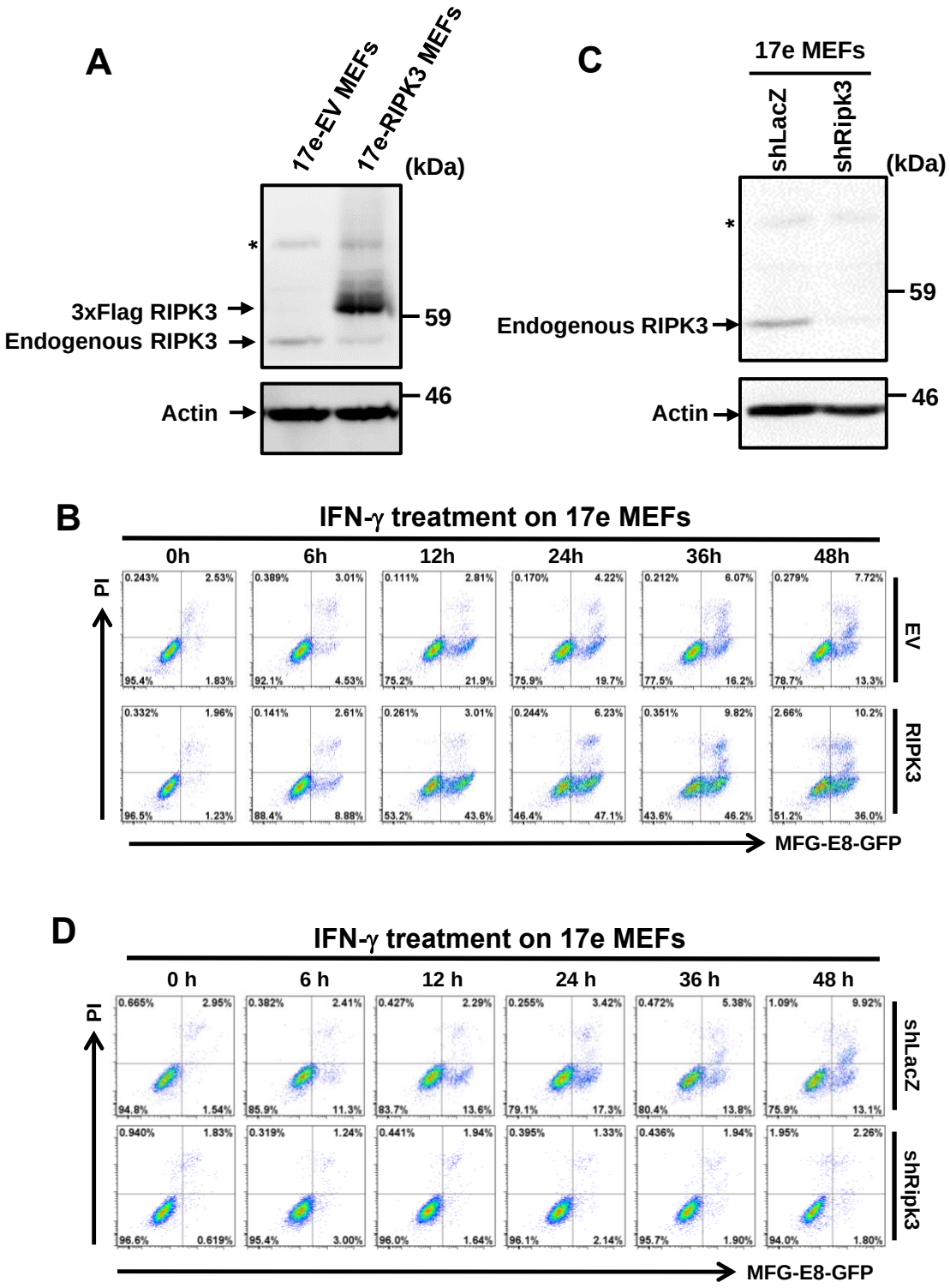

Figure 12. IFN-γ-induced PS exposure of 17e MEFs is affected by the expression level of RIPK3. **A**, 17e MEFs harboring the indicated expression vectors were analyzed by Western blotting with anti-RIPK3 and anti-actin antibodies. EV: an empty vector. **B**, 17e-EV MEFs or 17e-RIPK3 MEFs were treated with 10 ng/ml IFN-γ for the indicated periods. Cells were then stained with MFG-E8-GFP and PI, and analyzed by flow cytometry. **C**, 17e MEFs were infected with a lentiviral vector encoding shRNA for *Ripk3* (shRipk3) or *lacZ* (shLacZ). The expression levels of RIPK3 were analyzed by Western blotting with anti-RIPK3 and anti-actin antibodies. **D**, 17e MEFs expressing shLacZ or shRipk3 were treated with 10 ng/ml IFN-γ for the indicated periods. Cells were stained with MFG-E8-GFP and PI, and analyzed by flow cytometry. *: Non-specific bands. Representative Western blotting data and flow cytometric plots of more than three experiments are shown.

3.3 IFN-γ-induced PS exposure is independent of TMEM16F

Recently, a calcium-dependent membrane-associated scramblase, TMEM16F, was found to transport phospholipids bidirectionally in the plasma membrane, and activation of TMEM16F was reported to expose PS in a caspase-independent manner (9). Therefore, to further study the mechanism of IFN-γ-induced PS exposure, we next investigated whether TMEM16F is involved in the induction of IFN-γ-induced PS exposure.

3.3.1 Knockdown of TMEM16F in iC8KO-RIPK3 MEFs

I generated TMEM16F knockdown iC8KO-RIPK3 MEFs by expressing a shRNA specific for *Tmem16F* (sh16F). qRT-PCR (Fig. 13A) and Western blotting (Fig. 13B) analyses showed that the sh16F efficiently reduced the expression of TMEM16F at both mRNA and protein levels.

3.3.2 TMEM16F knockdown iC8KO-RIPK3 MEFs still manifested induction of PS exposure and necroptosis in response to IFN-γ

To analyze IFN-γ-induced PS exposure and necroptotic cell death in TMEM16F knockdown iC8KO-RIPK3 MEFs, IFN-γ-treated cells were analyzed by fluorescence microscopy (Fig. 14A) and flow cytometry (Fig. 14B). I found that the down-regulated expression of TMEM16F in iC8KO-RIPK3 MEFs neither abolished the PS exposure nor inhibited cell death after IFN-γ treatment (Fig. 14C). As well as the shLacZ-expressing iC8KO-RIPK3 MEF control, PS was exposed prior to the induction of necroptotic cell death in sh16F-expressing iC8KO-RIPK3 MEFs, indicating that the scramblase TMEM16F was not involved in the IFN-γ-induced PS exposure.

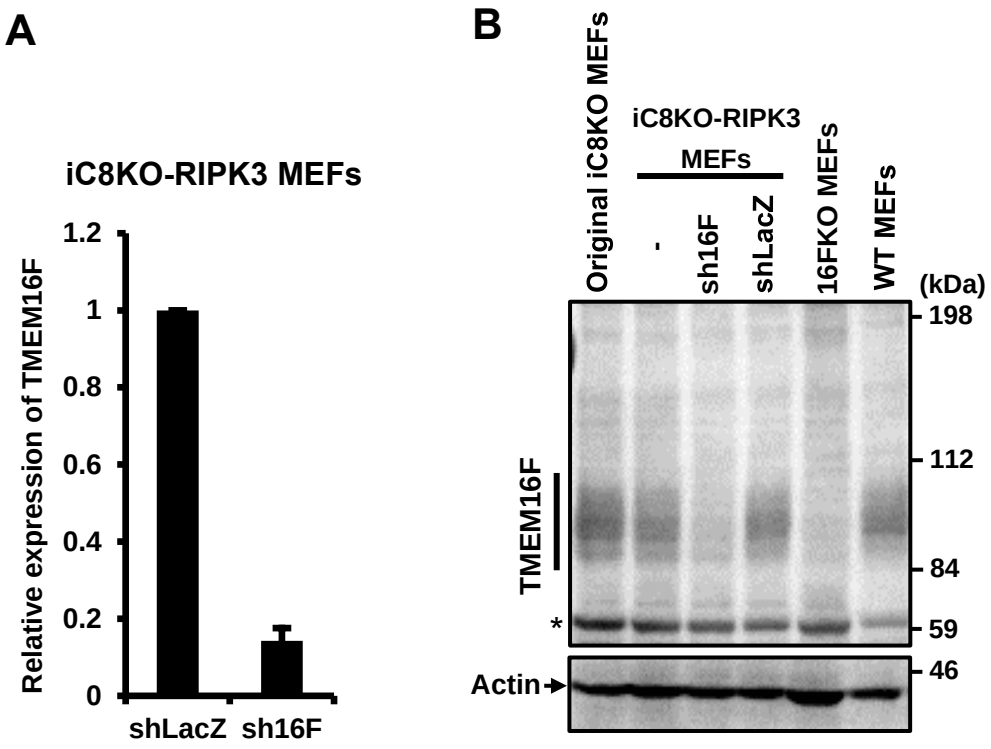

Figure 13. TMEM16F was knocked down by expression of *Tmem16F*-specific shRNA. **A** and **B**, iC8KO-RIPK3 MEFs were infected with a lentiviral vector encoding shRNA for *Tmem16F* (sh16F). The expression of TMEM16F was quantified by qRT-PCR (**A**), and Western blotting with anti-TMEM16F and anti-actin antibodies (**B**). *: Non-specific bands. Representative qRT-PCR data and Western blotting data of more than three experiments are shown. For qRT-PCR analysis, data are presented as mean ± S.D. (n≥3)

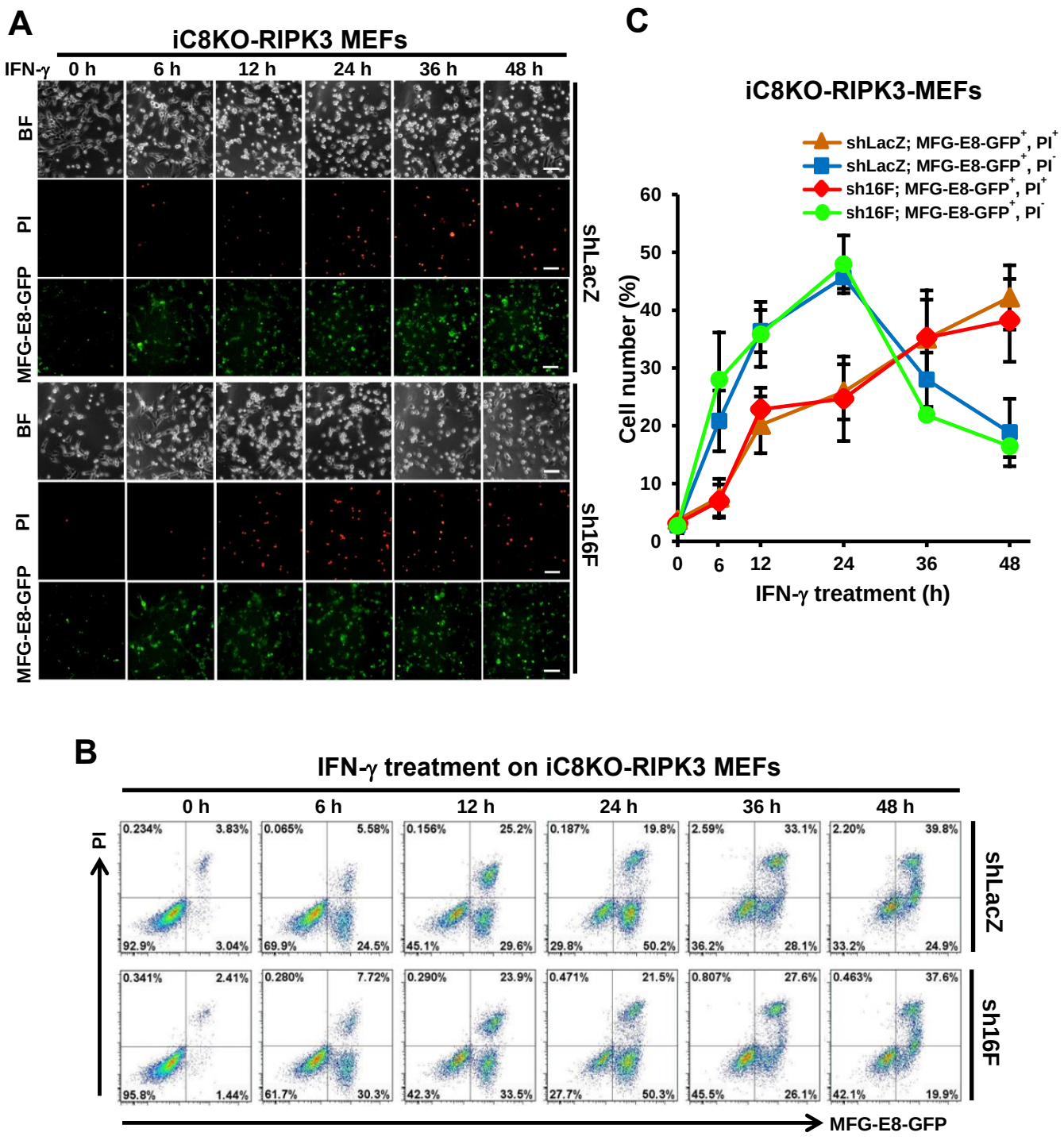

Figure 14. TMEM16F knockdown iC8KO-RIPK3 MEFs are still sensitive to IFN-γ.
A and **B**, iC8KO-RIPK3 MEFs expressing shLacZ or sh16F were treated with 10 ng/ml IFN-γ for the indicated periods. Cells were stained with MFG-E8-GFP and PI, and analyzed by fluorescence microscopy (**A**) and flow cytometry (**B**). Scale bars represent 100 μm. **C**, the data of the flow cytometric analysis (**B**) were graphically shown. Representative fluorescence images and flow cytometric plots of more than three experiments are shown. For flow cytometry quantification, data are presented as mean ± S.D. (n≥3)

3.4 MLKL is an indispensable factor for IFN-γ-induced PS exposure

As a key molecule in the execution of necroptosis, MLKL was recently identified to be a downstream substrate of RIPK3 (25, 49). After phosphorylation by RIPK3 (26), MLKL was reported to translocate to the plasma membrane and cause necroptotic membrane disruption (50). Therefore, I next investigated whether MLKL is a potential executive factor for the exposure of PS.

3.4.1 Knockdown of MLKL in iC8KO-RIPK3 MEFs using two different shRNAs specific for *Mlkl*

I also knocked down MLKL in iC8KO MEFs by expressing a shRNA specific for *Mlkl*. Two shRNAs, shMlkl#1 and shMlkl#2, were designed and utilized for knockdown of MLKL expression. The expression of MLKL was shown to be significantly down-regulated at both the mRNA and protein levels (Fig. 15, A and B) by the expression of the designed shRNAs.

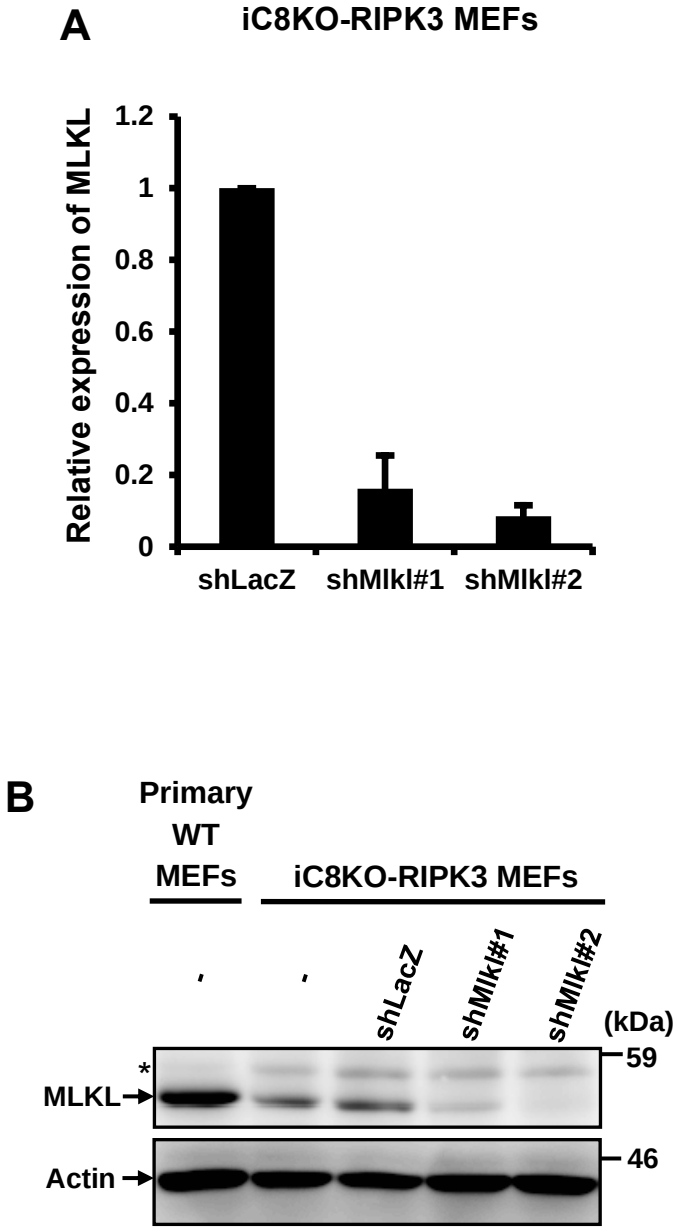

Figure 15. MLKLwas knocked down by expression of MLKL-specific shRNAs.
A and **B**, iC8KO-RIPK3 MEFs were infected with lentiviral vectors encoding two different shRNAs for MLKL (shMlkl#1 and shMlkl#2). The expression levels of MLKL were analyzed by qRT-PCR (**A)** and by Western blotting with anti-MLKL and anti-actin antibodies (**B**). *: Non-specific bands. Representative qRT-PCR data and Western blotting data of more than three experiments are shown. For qRT-PCR analysis, data are presented as mean ± S.D. (n≥3).

3.4.2 shMlkl#2-expressing iC8KO-RIPK3 MEFs are resistant to IFN-γ-induced PS exposure and cell death

Since the MLKL knockdown efficiency by shMlkl#2 was higher than that by shMlkl#1 (Fig. 15, A and B), I focused on the analysis of shMlkl#2-expressing iC8KO-RIPK3 MEFs. Cells were subjected to IFN-γ treatment, and the PS-exposing cells and dead cells were monitored by fluorescence microscopy (Fig. 16A) or flow cytometry (Fig. 16B). The quantified data (Fig. 16C) showed that the shMlkl#2-expressing iC8KO-RIPK3 MEFs neither exposed PS nor died after IFN-γ treatment, even when treated for a long period (48 h), indicating that the PS-exposing property was abolished by the down-regulation of MLKL.

3.4.3 shMlkl#1-expressing iC8KO-RIPK3 MEFs are also resistant to IFN-γ-induced PS exposure and cell death

I found that a moderate expression of residual MLKL was left in shMlkl#1-expressing iC8KO-RIPK3 MEFs. Therefore, to make clear whether the moderate expression of residual MLKL can sensitize iC8KO-RIPK3 MEFs to IFN-γ, shMlkl#1-expressing iC8KO-RIPK3 MEFs were subjected to IFN-γ treatment, and the PS-exposing cells and dead cells were monitored by flow cytometry (Fig. 17A). shMlkl#1-expressing iC8KO-RIPK3 MEFs also lost their PS-exposing property and sensitivity to IFN-γ treatment (Fig. 17B), indicating that the moderate expression of residual MLKL is not sufficient to induce PS exposure and necroptosis in iC8KO-RIPK3 MEFs. Taken together, MLKL is essential for IFN-γ-induced PS exposure.

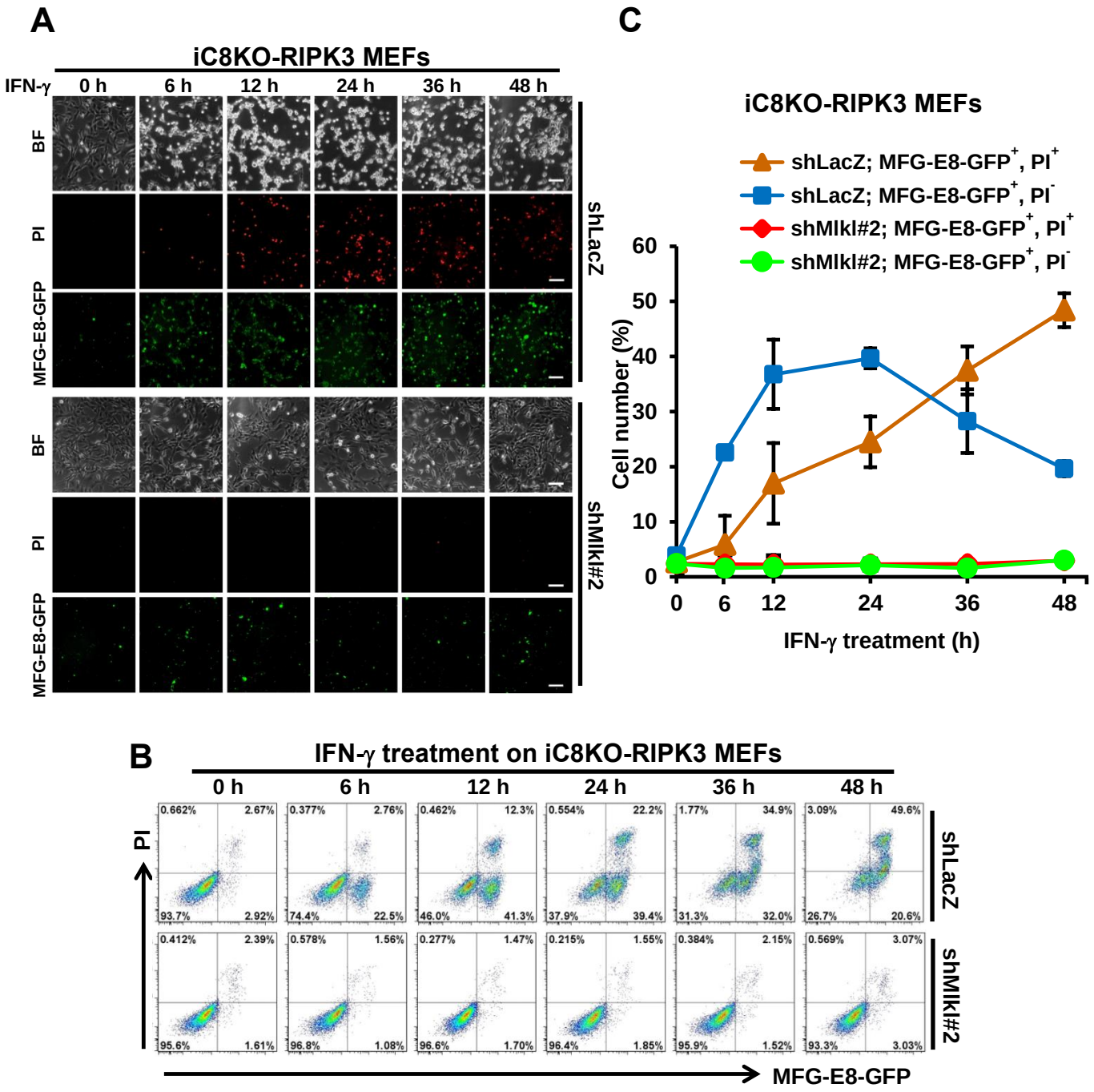

Figure 16. MLKL-downregulated iC8KO-RIPK3 MEFs are resistant to IFN-γ-induced PS exposure and necroptosis.

A and **B**, iC8KO-RIPK3 MEFs expressing shLacZ or shMlkl#2 were treated with 10 ng/ml IFN-γ for the indicated periods. Cells were stained with MFG-E8-GFP and PI, and analyzed by fluorescence microscopy (**A**) and flow cytometry (**B**). **C**, the data of the flow cytometric analysis (**B**) are graphically shown. Representative fluorescence images and flow cytometric plots of more than three experiments are shown. For flow cytometry quantification, data are presented as mean ± S.D. (n≥3).

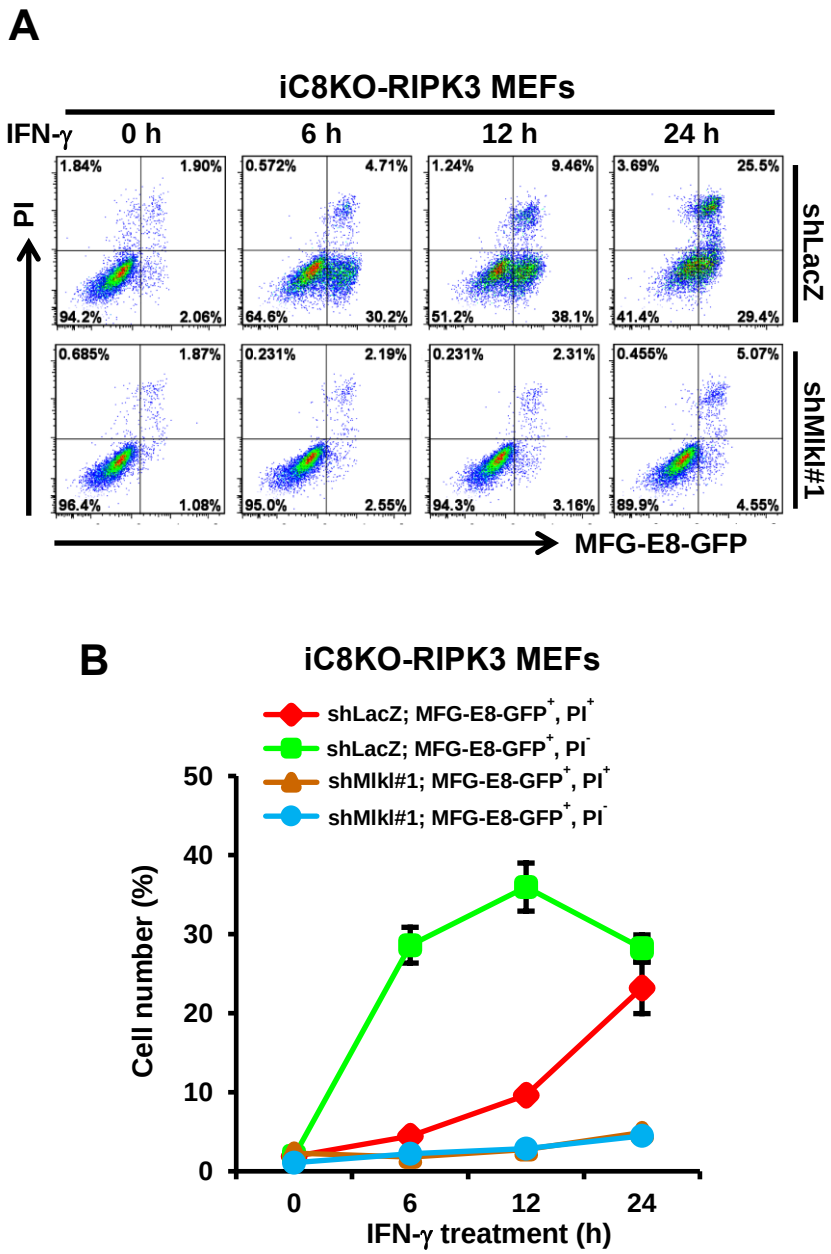

Figure 17. shMlkl#1-expressing iC8KO-RIPK3 MEFs are also resistant to IFN-γ-induced PS exposure and necroptosis.

A, iC8KO-RIPK3 MEFs infected with shLacZ or shMlkl#1 were treated with 10 ng/ml IFN-γ for the indicated periods. Cells were stained with MFG-E8-GFP and PI, and analyzed by flow cytometry. **B**, the data of the flow cytometric analysis (**A**) are graphically shown. Representative flow cytometric plots of more than three experiments are shown. For flow cytometry quantification, data are presented as mean ± S.D. (n≥3).

3.5 MLKL is phosphorylated and oligomerized in IFN-γ-treated MEFs in the absence of caspase-8 activity

In TNF-induced necroptosis, MLKL was recently reported to be phosphorylated by RIPK3 to form an oligomer and translocate to the plasma membrane where it disrupts membrane integrity, resulting in necroptotic cell death (26, 51, 52). In my IFN-γ-induced necroptosis system, I also supposed that MLKL is oligomerized after phosphorylation by RIPK3 and is involved in the PS-exposing mechanism in MEFs. Then, I analyzed MLKL oligomerization in IFN-γ-induced PS-exposing MEFs.

3.5.1 MLKL is phosphorylated in IFN-γ-treated MEFs in the absence of caspase-8 activity

To confirm whether MLKL was activated by RIPK3, phosphorylation of MLKL in primary WT MEFs (Fig. 18A) or in iC8KO-RIPK3 MEFs (Fig. 18B) after treatment with IFN-γ and z-VAD-fmk (IZ) or only IFN-γ, respectively, was analyzed by Western blotting. I found that phosphorylation of MLKL began to be detected after 6 h IZ treatment or 3 h IFN-γ treatment in primary WT MEFs or in iC8KO-RIPK3 MEFs, respectively. Not only the amounts of phosphorylated MLKL (pMLKL) but also the total amounts of MLKL increased in a time-dependent manner after IFN-γ treatment.

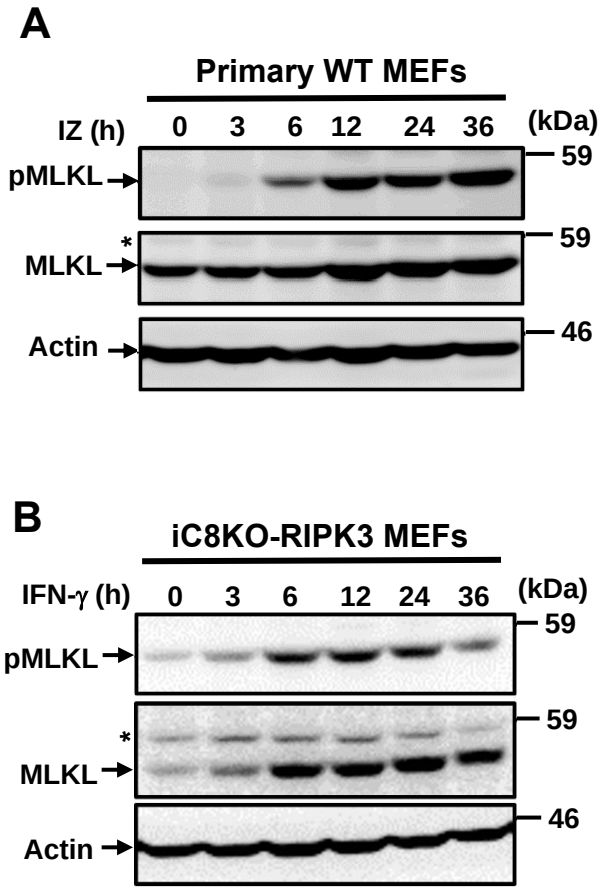

Figure 18. Phosphorylation of MLKL in IFN-γ-induced PS-exposing MEFs. **A** and **B**, primary WT MEFs (**A**) and iC8KO-RIPK3 MEFs (**B**) were treated with 10 ng/ml IFN-γ and 50 μM z-VAD-fmk (IZ) and with only 10 ng/ml IFN-γ, respectively, for the indicated periods. Cell lysates were resolved on reducing SDS-PAGE and analyzed by Western blotting with anti-phosphorylated MLKL (pMLKL), anti-MLKL and anti-actin antibodies. *: Non-specific bands. Representative Western blotting data of more than three experiments are shown.

3.5.2 MLKL oligomerizes in IFN-γ-treated MEFs in the absence of caspase-8 activity

To investigate whether the oligomerization of activated MLKL protein was induced in IFN-γ-treated MEFs exposing PS, primary WT MEFs were subjected to IZ treatment. The expression levels and oligomerization of MLKL were analyzed by reducing and non-reducing SDS-PAGE, respectively, as described in Chapter 2, Materials and methods, section 2.6. I found that the bands of MLKL monomer were detected at a molecular weight (Mr) of approximately 52 kDa under reducing conditions, increased in a time dependent manner. Under non-reducing conditions, bands of MLKL oligomer with Mr of approximately 160 kDa were detectable, and also increased in intensity in a time-dependent manner. The Mr of the MLKL oligomer was roughly three times that of the MLKL monomer (Fig. 19A), suggesting that the MLKL oligomers were trimers. These bands of MLKL monomer and trimer were similarly observed in IFN-γ-treated iC8KO-RIPK3 MEFs (Fig. 19B), whereas not observed in IFN-γ-treated shMlkl#2-expressing iC8KO-RIPK3 MEFs (Fig. 19C). On the other hand, the bands of both MLKL monomer and trimer were detected in TNF-α, cycloheximide, and z-VAD-fmk (TCZ)-treated primary WT MEFs (Fig. 19D); however, their expression levels decreased rapidly within 12 h in a time-dependent manner, in contrast to IZ-treated primary WT MEFs, in which MLKL monomer and trimer expression levels increased between 3 and 24 h. All the data indicate that IFN-γ, but not TNF-α induces the expression of MLKL in MEFs in the absence of caspase-8 activity.

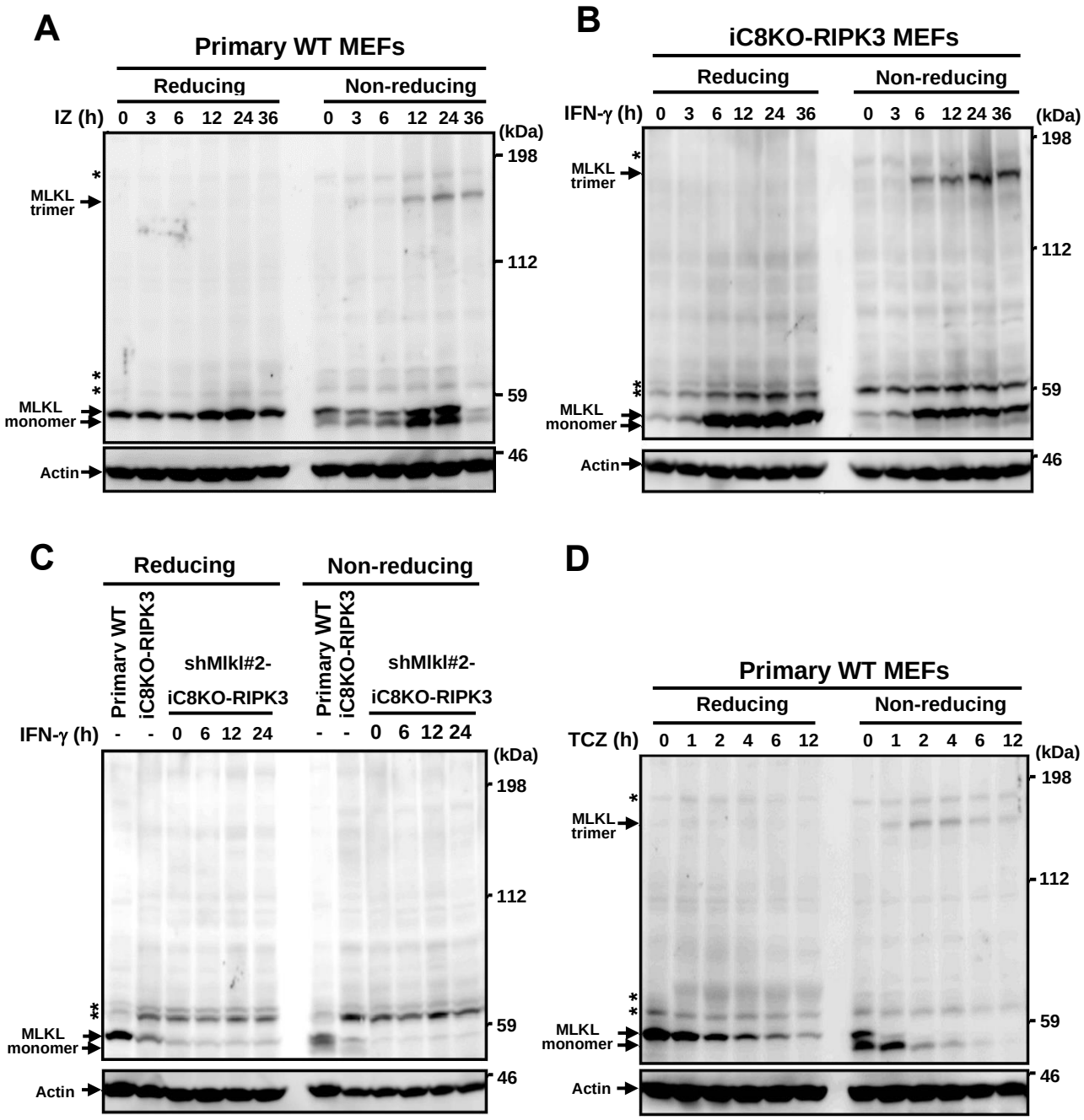

Figure 19. Oligomerization of MLKL in IFN-γ-treated MEFs in the absence of caspase-8 activity. **A** and **B**, cell lysates from primary WT MEFs treated with 10 ng/ml IFN-γ and 50 μM z-VAD-fmk (IZ) (**A**) and iC8KO-RIPK3 MEFs treated with 10 ng/ml IFN-γ (**B**) for the indicated periods, were resolved on reducing or non-reducing SDS-PAGE and analyzed by Western blotting with anti-MLKL and anti-actin antibodies. **C**, primary WT MEFs, iC8KO-RIPK3 MEFs, and shMlkl#2-expressing iC8KO-RIPK3 MEFs were treated with 10 ng/ml IFN-γ for the indicated periods. Cell lysates were resolved on reducing or non-reducing SDS-PAGE and analyzed by Western blotting with anti-MLKL and anti-actin antibodies. **D**, cell lysates from primary WT MEFs treated with 10 ng/ml TNF-α, 1 μg/ml cycloheximide, and 50 μM z-VAD-fmk (TCZ) for the indicated periods, were resolved on reducing or non-reducing SDS-PAGE and analyzed by Western blotting with anti-MLKL and anti-actin antibodies. *: Non-specific bands. Representative Western blotting data of more than three experiments are shown.

3.5.3 Oligomerized MLKL is also phosphorylated in IFN-γ-treated MEFs in the absence of caspase-8 activity

Since phosphorylation of MLKL was reported to be required for its oligomerization in the TNF-induced necroptosis, and the phosphorylated state in MLKL oligomers was maintained during the necroptotic process (26), I was interested in whether the oligomerized MLKL is phosphorylated in the PS-exposing MEFs after treatment with IFN-γ. Therefore, the phosphorylation of the oligomerized MLKL in IFN-γ-treated MEFs was analyzed by Western blotting. As shown in Fig. 20, A and B, upper panels, the bands of MLKL oligomer were detected as phosphorylated MLKL, and their phosphorylation levels increased in a time dependent manner both in IZ-treated primary WT MEFs and IFN-γ-treated iC8KO-RIPK3 MEFs, implying that the MLKL monomers oligomerized after activation by RIPK3, and the phosphorylated MLKL oligomers might function in the PS exposure in my IFN-γ-induced necroptosis system.

3.5.4 Oligomerization of MLKL is not induced, but slight phosphorylation of MLKL monomer is induced in IFN-γ-treated iC8KO-RIPK3 RHIM mutant MEFs

Phosphorylation and oligomerization of MLKL protein in iC8KO expressing RIPK3 RHIM domain mutant (iC8KO-RIPK3 RHIM mutant) MEFs were also investigated after treatment with IFN-γ. As expected, the bands of MLKL oligomers were not detected in iC8KO-RIPK3 RHIM mutant MEFs under non-reducing conditions (Fig. 21, lower panels), indicating that the interaction of RIPK3 and RIPK1 through their RHIM domain is crucial for activation and oligomerization of MLKL. However, interestingly, slightly phosphorylated bands of MLKL were observed in iC8KO-RIPK3 RHIM mutant MEFs after treatment with IFN-γ under reducing conditions (Fig. 21, upper panels). Importantly, the phosphorylation level of MLKL was much lower than that of iC8KO MEFs expressing WT RIPK3, implying that MLKL is still activated at a low level, which is not enough to trigger the oligomerization.

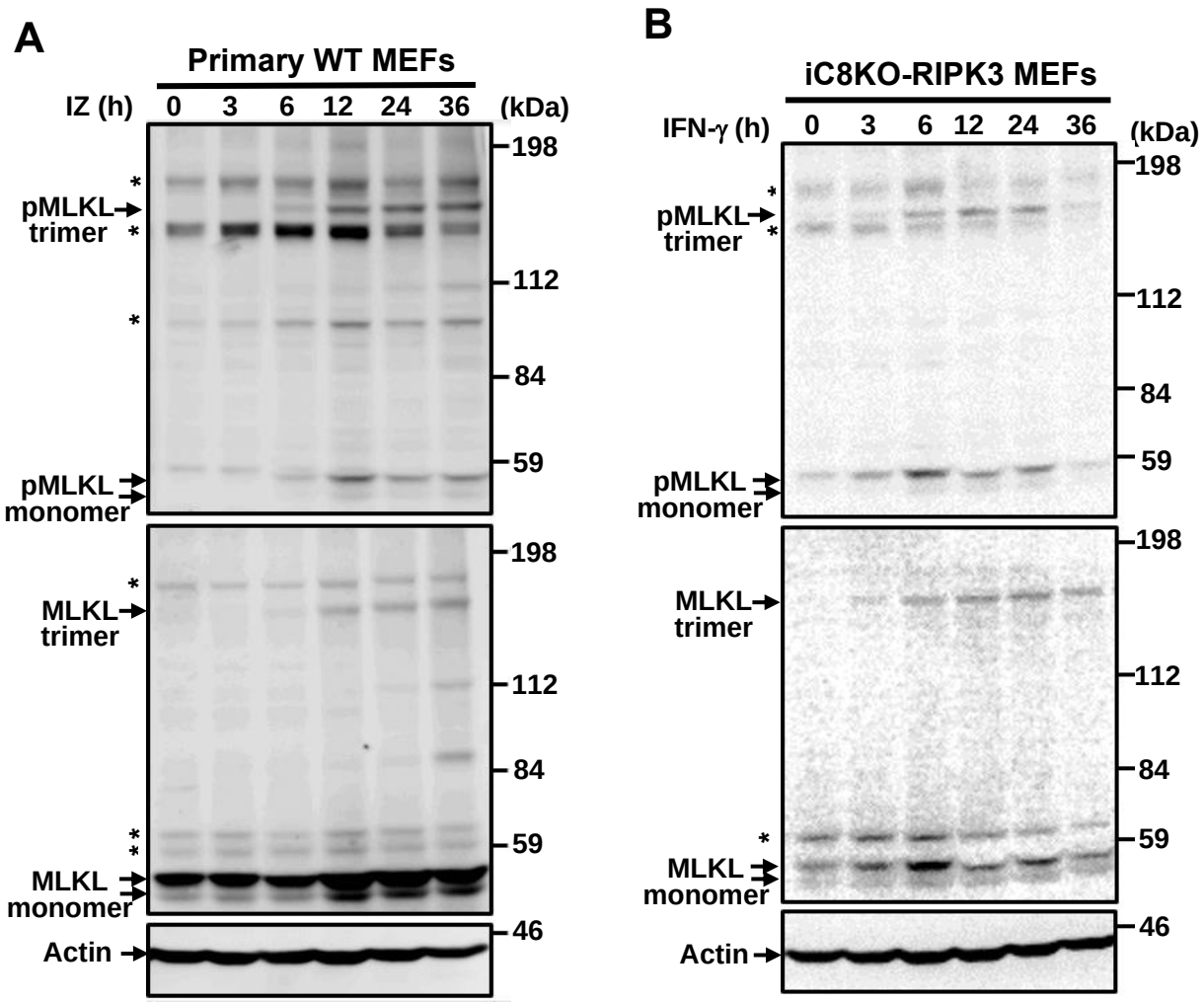

Figure 20. MLKL oligomers are phosphorylated in IFN-γ-treated MEFs in the absence of caspase-8 activity.

A and **B**, primary WT MEFs (**A**) and iC8KO-RIPK3 MEFs (**B**) were treated with 10 ng/ml IFN-γ and 50 μM z-VAD-fmk (IZ) and 10 ng/ml IFN-γ, respectively, for the indicated periods. Cell lysates were resolved on non-reducing SDS-PAGE and analyzed by Western blotting with anti-MLKL, anti-phosphorylated MLKL (pMLKL) and anti-actin antibodies. *: Non-specific bands. Representative Western blotting data of more than three experiments are shown.

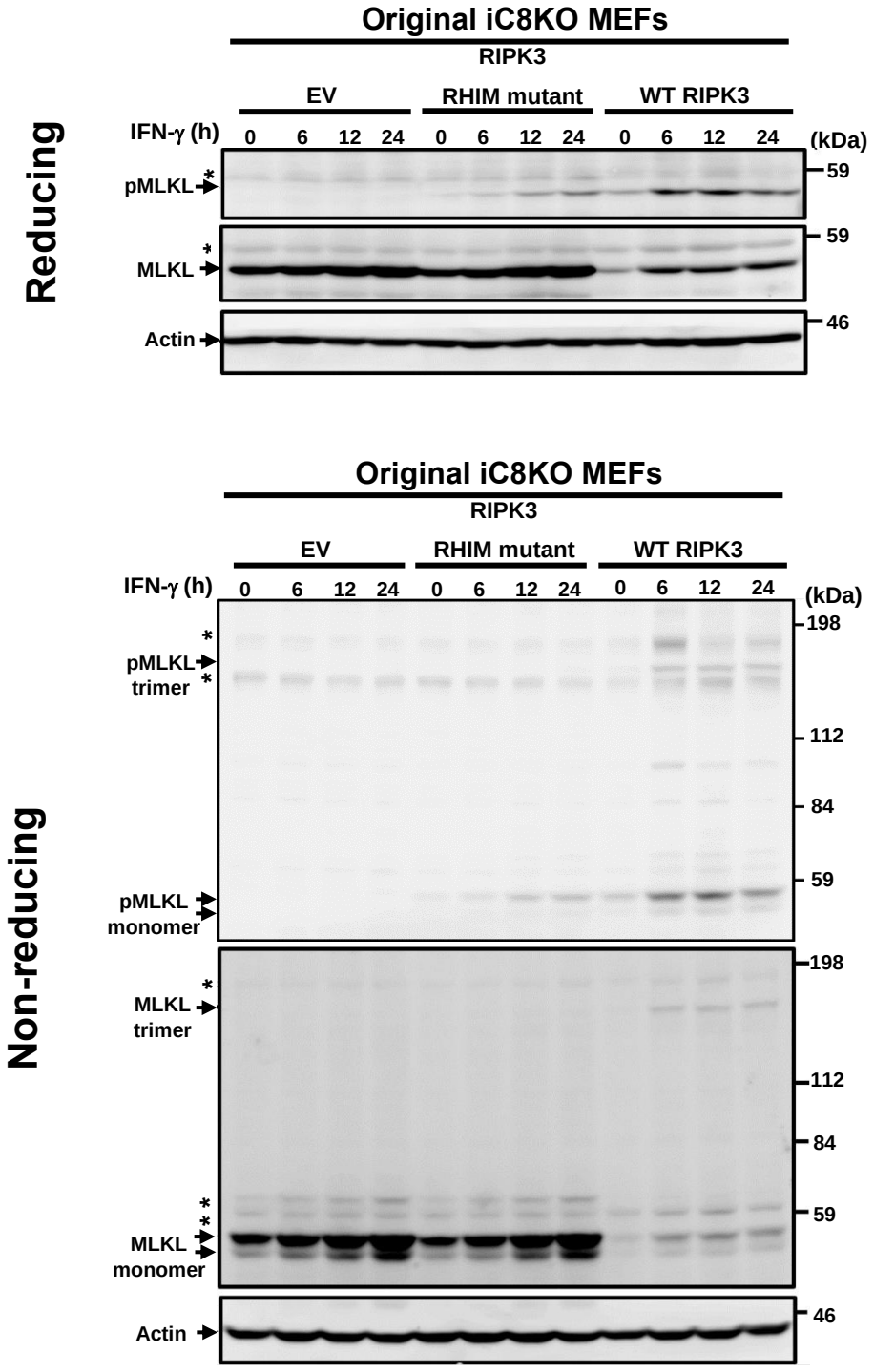

Figure 21. Phosphorylation and oligomerization of MLKL in IFN-γ-treated iC8KO-RIPK3 RHIM mutant MEFs.

The original iC8KO MEFs harboring the indicated expression vectors were treated with 10 ng/ml IFN-γ for the indicated periods. Cell lysates were then collected and resolved on reducing or non-reducing SDS-PAGE, and analyzed by Western blotting with anti-MLKL, anti-phosphorylated MLKL (pMLKL), and anti-actin antibodies. EV: an empty vector. *: Non-specific bands. Representative Western blotting data of more than three experiments are shown.

3.6 Plasma membrane bubbles with exposed PS are formed and shed from PS-exposing cells during IFN-γ-induced necroptosis

MLKL was reported to oligomerize and translocate to the plasma membrane after activation by RIPK3 in TNF-induced necroptosis (28, 51), and similar processes were observed in my IFN-γ-induced necroptosis model. I then investigated the behavior of exposed PS on the plasma membrane before the loss of membrane integrity in IFN-γ-treated iC8KO-RIPK3 MEFs (Fig. 22). After treatment with IFN-γ for 6 h, not only PS exposure but also MFG-E8-GFP-positive (MFG-E8-GFP^{+}) bubble formation was found on the plasma membrane of iC8KO-RIPK3 MEFs. These bubbles were still detectable and appeared to be shed from the cell surface after 24 h IFN-γ treatment. Since IFN-γ-induced formation and shedding of PS-exposing bubbles were similar to those recently reported to be induced by TNF (26, 31, 53), I speculated that these PS-exposing bubbles induced by IFN-γ may also contain activated MLKL, similar to TNF-α-induced bubbles, and might be released from cells to maintain the low level of activated MLKL which is sufficient to induce PS exposure, but not enough to disrupt membrane integrity.

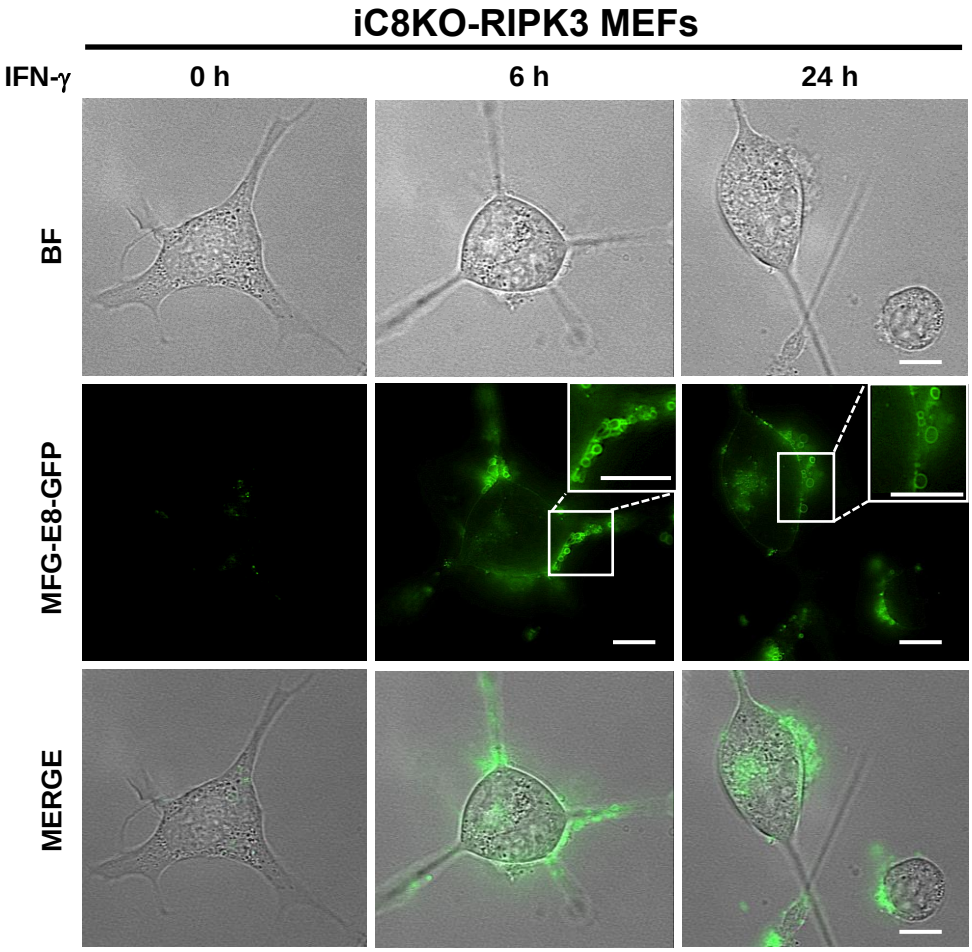

Figure 22. Formation and shedding of membrane bubbles in IFN-γ-treated iC8KO-RIPK3 MEFs.
iC8KO-RIPK3 MEFs were treated with 10 ng/ml IFN-γ for the indicated periods and then directly stained with MFG-E8-GFP. Cells were then observed by fluorescence microscopy. Scale bars represent 10 μm. Representative fluorescence images of more than three experiments are shown.

3.7 PS-exposing MEFs are not committed to die in IFN-γ-induced necroptosis

Oligomerization of activated MLKL is crucial for PS exposure and execution of necroptosis in MEFs. Therefore, I investigated whether the IFN-γ-induced PS-exposing MEFs with activated MLKL are committed to die or can survive after removing IFN-γ.

3.7.1 IFN-γ-treated MEFs exposing PS are resuscitated to survive and begin to grow after removing IFN-γ

PS exposure was induced by 6 h treatment with IFN-γ on iC8KO-RIPK3 MEFs, MEFs were then washed with pre-warmed PBS, termed "washing out", to remove the remaining IFN-γ interacting with IFN-γ receptors. The PS-exposing cells were then cultured in fresh culture medium without IFN-γ. Viable cells and dead cells after removal of IFN-γ were analyzed by cell counting using the trypan blue exclusion method. As expected, PS-exposing MEFs without washing out IFN-γ did not grow and progressed to necroptosis (Fig. 23, A and B), whereas after removal of IFN-γ, PS-exposing MEFs cultured without IFN-γ resumed to grow and did not die.

3.7.2 IFN-γ-induced PS exposure is observed in MEFs during a significant period after removal of IFN-γ

IFN-γ was removed from iC8KO-RIPK3 MEFs after 6 h treatment with IFN-γ, cells were cultured without IFN-γ as described in Figure 23, and PS-exposing and dead cells were then analyzed by flow cytometry. As shown in Fig. 24, A and B, the number of PS-negative living (MFG-E8-GFP$^-$PI$^-$) cells began to increase at 6 h after removing IFN-γ. In contrast, the number of PS-positive living (MFG-E8-GFP$^+$PI$^-$) cells continued to increase for a further 6 h after removing IFN-γ. These data suggest that the signal for induction of PS exposure, but not for induction of necroptotic cell death, from the oligomerized MLKL was still active for at least 6 h after removing IFN-γ.

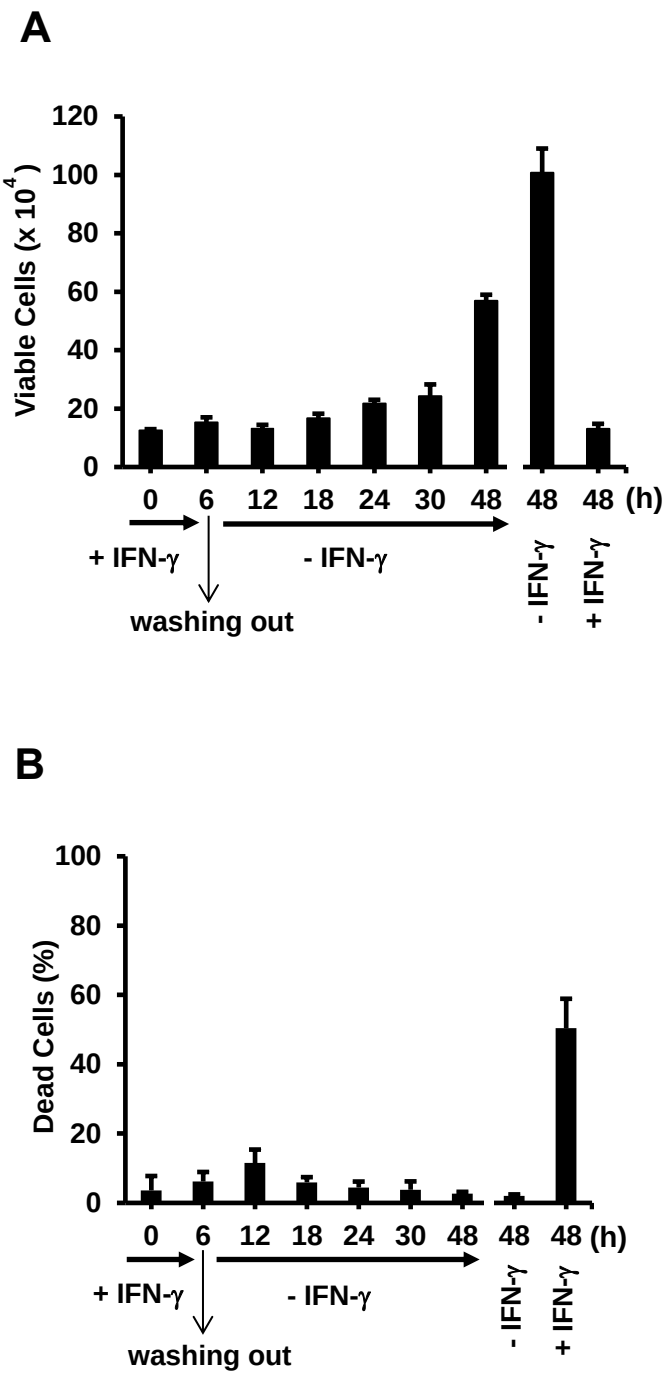

Figure 23. Analysis of cell growth and cell death in IFN-γ-treated iC8KO-RIPK3 MEFs after removal of IFN-γ.

A and **B**, after iC8KO-RIPK3 MEFs were treated with 10 ng/ml IFN-γ for 6 h, IFN-γ was removed, and cells were washed well with pre-warmed PBS. Cells were then cultured with new culture medium without IFN-γ for the indicated periods, and the numbers of viable cells (cell growth) (**A**) and dead cells (cell death) (**B**) were quantified by the trypan blue exclusion method using a hemocytometer. Representative data of more than three experiments are shown. All the data are presented as mean ± S.D. (n≥3).

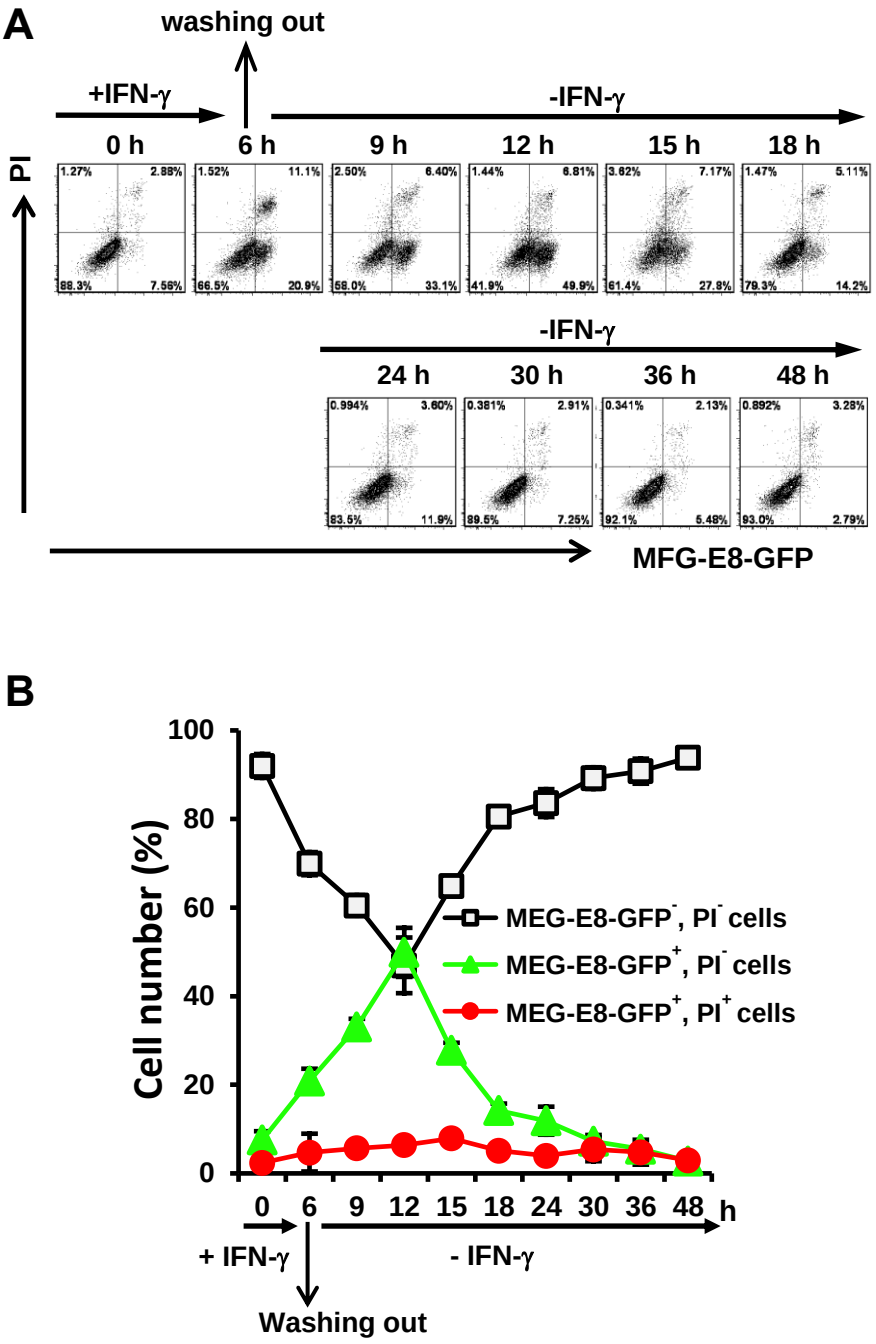

Figure 24. IFN-γ induces PS exposure without the induction of necroptotic cell death. **A**, after a treatment with 10 ng/ml IFN-γ on iC8KO-RIPK3 MEFs for 6 h, IFN-γ was removed, cells were washed with pre-warmed PBS twice and then cultured with fresh culture medium for the indicated periods. Cells at the indicated time points were stained with MFG-E8-GFP and PI, and then analyzed by flow cytometry. **B**, the data of the flow cytometric analysis (**A**) are graphically shown. Representative flow cytometric plots of more than three experiments are shown. For flow cytometry quantification, data are presented as mean ± S.D. (n≥3)

3.7.3 Resuscitated MEFs after removal of IFN-γ are still sensitive to IFN-γ treatment

To further analyze the characteristics of the resuscitated MEFs after removing IFN-γ, PS-positive living (MFG-E8-GFP^{+}PI^{-}) iC8KO-RIPK3 MEFs were sorted 6 h after IFN-γ treatment by FACS (fluorescence-activated cell sorting) (Fig. 25A, left panel). Approximately 80% of the sorted cells were confirmed to be PS-positive living cells. These sorted cells were then cultured without IFN-γ. After 12 h or 2 days cultivation, more than 80% of the total cells became PS-negative living (MFG-E8-GFP^{-}PI^{-}) cells (Fig. 25A, right panel), indicating that the sorted PS-positive living (MFG-E8-GFP^{+}PI^{-}) cells progressed to normal living cells after removal of IFN-γ. And, in addition, these recovered cells still manifested induction of PS exposure in response to IFN-γ after 6 h IFN-γ treatment (Fig. 25B), as well as their parental iC8KO-RIPK3 MEFs (Fig. 24). Taken together, these results indicated that living PS-exposing iC8KO-RIPK3 MEFs were able to be resuscitated to normal PS-negative living MEFs when the IFN-γ-induced signal responsible for activation of MLKL was removed.

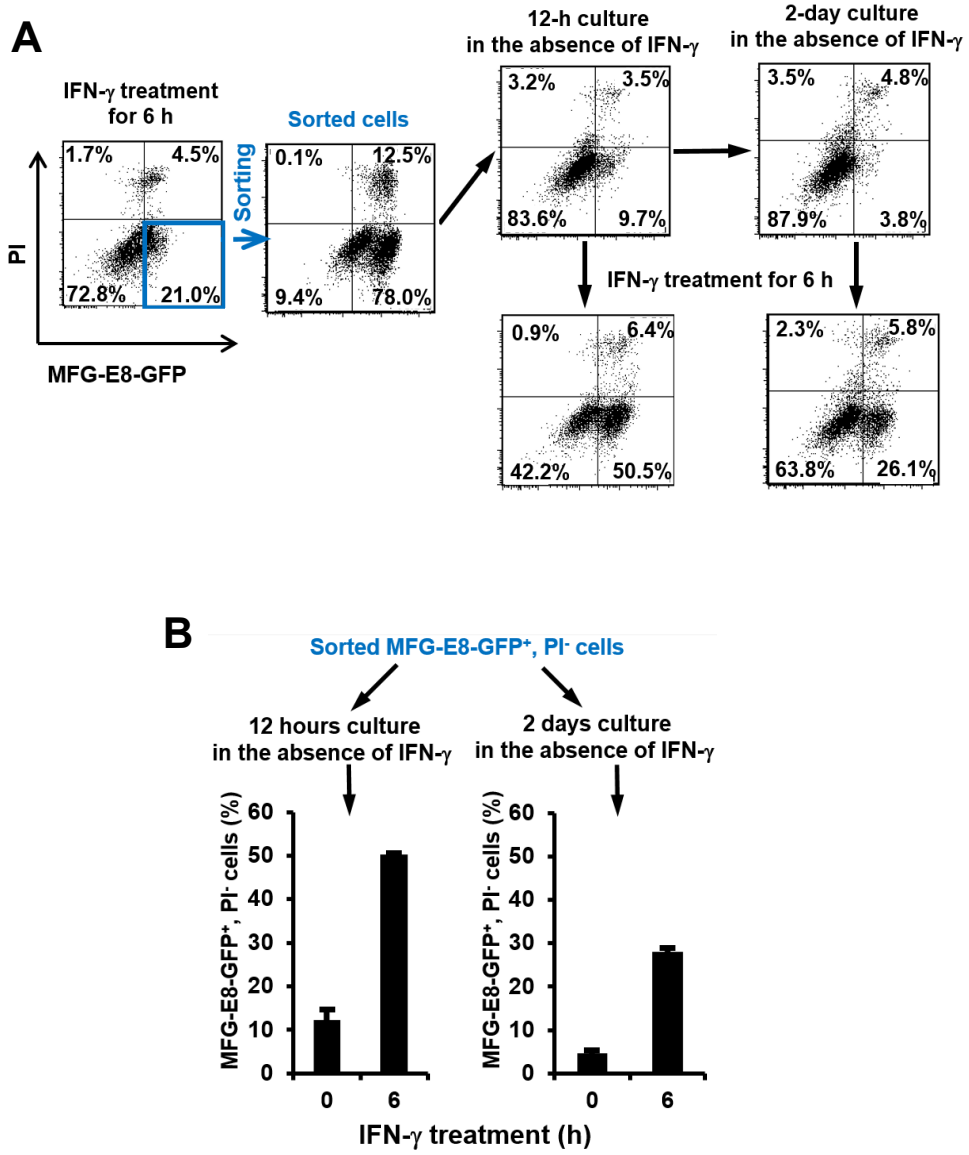

Figure 25. Resuscitation of IFN-γ-induced PS-exposing iC8KO-RIPK3 MEFs by removal of IFN-γ.

A, after 6 h treatment with 10 ng/ml IFN-γ on iC8KO-RIPK3 MEFs, cells were stained with MFG-E8-GFP and PI, and the MFG-E8-GFP^{+}PI^{-} cells shown in the blue square were sorted and immediately analyzed by flow cytometry. Sorted cells were cultured without IFN-γ for 12 h or 2 days and analyzed by flow cytometry after staining with MFG-E8-GFP and PI. PS exposure in the sorted cells after cultivation without IFN-γ for 12 h and 2 days was again assessed by flow cytometry after a treatment with 10 ng/ml IFN-γ for 6 h. **B**, the data of the flow cytometric analysis (**A**) are graphically shown. Representative flow cytometric plots of more than three experiments are shown. For flow cytometry quantification, data are presented as mean ± S.D. (n≥3)

3.8 IFN-γ also induced PS exposure in human cells

In this study, IFN-γ-induced PS exposure was found in mouse cells in the absence of caspase-8 activity. I wondered whether the same phenomenon could be observed in human cells, and next investigated the IFN-γ-induced PS exposure in human cells.

3.8.1 IFN-γ induced PS exposure in human HT29 cells in the presence of Smac mimetics and z-VAD-fmk

Since IFN-γ-induced necroptotic cell death was reported in human colorectal adenocarcinoma-derived HT29 cells in the presence of Smac mimetics (a synthetic antagonist to inhibitor of apoptosis protein/IAP) and z-VAD-fmk (35), I then analyzed the IFN-γ-induced PS exposure in HT29 cells. As expected, IFN-γ treatment together with Smac mimetics and z-VAD-fmk (ISZ) also induced PS exposure prior to the induction of necroptotic cell death in HT29 (Fig. 26). Both IFN-γ-induced PS exposure and necroptosis were inhibited by co-treatment with a human MLKL-specific inhibitor, necrosulfonamide (NSA) (52), indicating that IFN-γ-induced MLKL-dependent PS exposure is induced in not only MEFs but also human HT29 cells in the absence of caspase-8 activity.

3.8.2 IFN-γ also induced PS exposure prior to cell death in a novel type of cell death in human HT29 cells in the presence of Smac mimetics

Recently, a novel caspase-10- and RIPK1-dependent cell death was reported to be induced by a combination of IFN-γ and Smac mimetics (IS) in HT29 cells (54). I also investigated whether PS is exposed in this IS-induced novel cell death. As shown in Fig. 27, I found that PS exposure and cell death can be observed in HT29 cells and were shown to be time-dependent. However, both IS-induced PS exposure and cell death were shown to be insensitive to NSA (data no shown). Collectively, the mechanism of IS-induced PS exposure in HT29 cells seemed to differ from that observed in IZ-treated MEFs.

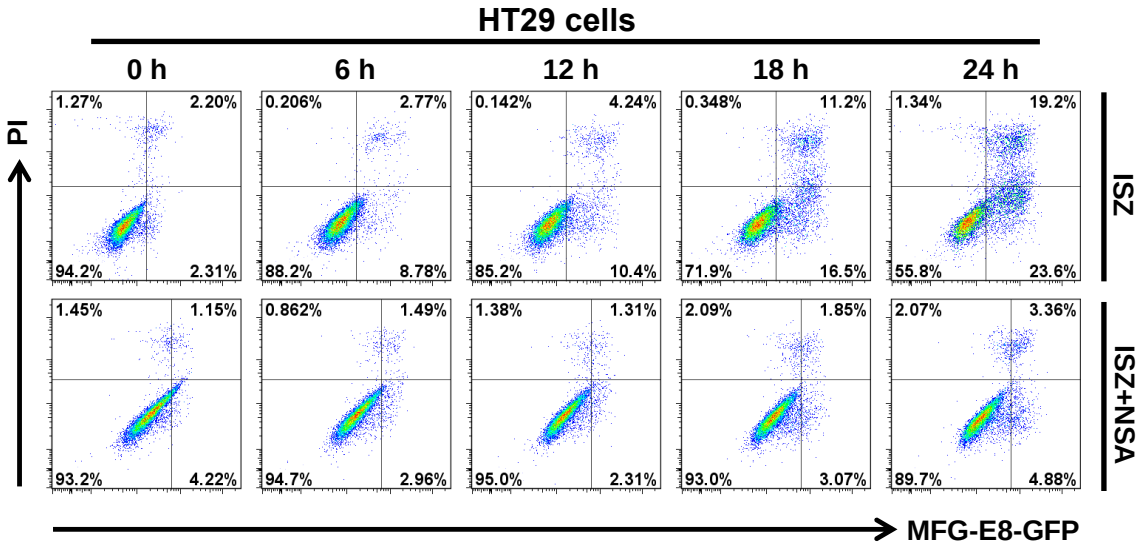

Figure 26. IFN-γ treatment together with Smac mimetics and z-VAD-fmk induces PS exposure and necroptosis in human HT29 cells.
Human HT29 cells were treated with 10 ng/ml human IFN-γ, 1 μM Smac mimetics, and 30 μM z-VAD-fmk (ISZ) in the presence or absence of necrosulfonamide (NSA) for the indicated periods. Cells were then stained with MFG-E8-GFP and PI, and analyzed by flow cytometry. Representative flow cytometric plots of more than three experiments are shown.

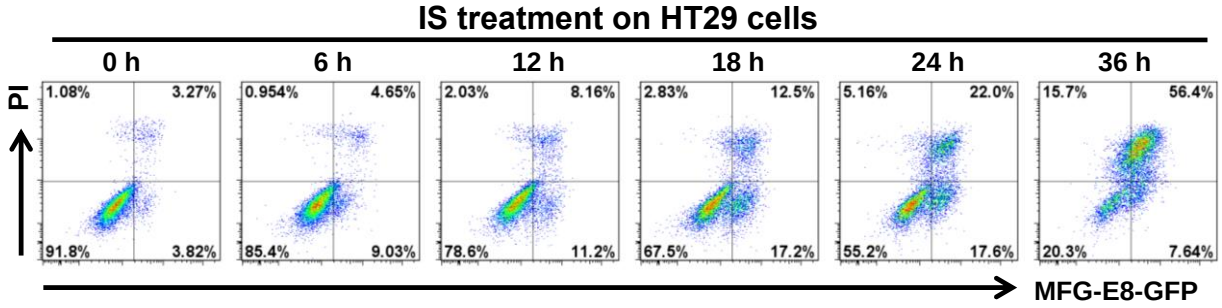

Figure 27. IFN-γ treatment together with Smac mimetics induces PS exposure and cell death in human HT29 cells.
Human HT29 cells were treated with 10 ng/ml human IFN-γ and 1 μM Smac mimetics (IS) for the indicated periods. Cells were then stained with MFG-E8-GFP and PI, and analyzed by flow cytometry. Representative flow cytometric plots of more than three experiments are shown.

Chapter 4

Discussion

4.1 Similarities and differences of PS exposure between apoptosis and necroptosis

The mechanism of PS exposure during apoptosis has been extensively studied (2, 4, 7). In the case of necrosis, PS exposure had been considered not to be induced; however, recent studies showed that PS can be exposed during TNF-induced necroptosis (30, 31) and the mechanism is still largely unknown. I found that IFN-γ induced not only necroptosis, but also PS exposure in caspase-8 negative MEFs. During the IFN-γ-induced necroptosis, PS was exposed prior to the induction of cell death, as with the PS exposure pattern of apoptosis (4, 55). However, IFN-γ-induced PS exposure is caspase-independent and MLKL-dependent, which completely differs from that of apoptosis. Moreover, PS exposure was induced by IFN-γ for at least 10 h before the induction of necroptosis, and most of the 6 h IFN-γ-treated cells exposing PS were not committed to die after removing IFN-γ (Figs. 23 and 24). Therefore, short-time IFN-γ treatment only induces PS exposure, but not necroptosis. IFN-γ-induced PS-exposing cells may also be engulfed by macrophages through phagocytotic clearance and enhance the inflammatory responses of PS receptor positive cells. The fate and biological significance of IFN-γ-treated cells exposing PS warrant further research.

4.2 Correlation between MLKL oligomer and PS exposure

My results demonstrated that MLKL trimer (oligomerized MLKL), an active form of MLKL, was formed at 6 h, and increased in a time-dependent manner after IFN-γ treatment (Fig. 19, A and B), in accord with the time-course of PS exposure observed in IFN-γ-treated MEFs (Fig. 5 and Fig. 8B). Activated (phosphorylated) MLKL was reported to oligomerize and translocate to the plasma membrane (28, 50, 51), and MLKL itself was also reported to have binding affinity for PS to some extent (26). Together with these previous data and my finding that the scramblase, TMEM16F, was not involved in the IFN-γ-induced PS exposure (Fig. 14), the MLKL trimer appears to be essential for PS exposure. Therefore, I speculated that the MLKL trimer may

function to indirectly (or possibly directly) externalize PS to the outer leaflet of the plasma membrane before execution of IFN-γ-induced necroptotic cell death.

4.3 The fate of MLKL expression in IFN-γ-induced necroptosis differs from that in TNF-induced necroptosis

Previous studies showed that the amount of MLKL protein decreased rapidly within 4 hours in MEFs after TNF treatment (51, 56). This rapid reduction of MLKL protein was further confirmed in my study (Fig. 19D). Intriguingly, in contrast to TNF stimulation, the MLKL protein (including monomer and trimer) level increased in a time-dependent manner from 3 h after IFN-γ treatment (Fig. 19). Downstream of the IFN-γ receptor, classical JAK/STAT signaling was reported to be utilized by IFN-γ to induce expression of pro-necrotic genes (e.g., RIPK1, PKR, and MLKL) and activate RIPK1/RIPK3-dependent necroptosis (57, 58). Therefore, in my IFN-γ-induced necroptosis model, IFN-γ may directly induce expression of MLKL, and the IFN-γ-activated pro-necrotic signaling pathway may work to promote PS exposure and subsequent necroptosis.

4.4 The amount of phosphorylated MLKL is crucial for MLKL oligomerization in IFN-γ-induced PS exposure and necroptosis

RIPK3 has been demonstrated to phosphorylate and activate MLKL during TNF-induced necroptosis (30, 38, 58, 59). In my study, RIPK3 was also demonstrated to be essential for IFN-γ-induced PS exposure and necroptosis (Fig. 8), and the interaction of RIPK3 with RIPK1 through their RHIM domains was crucial for the oligomerization of MLKL (Fig. 21). Consistent with this notion, slight phosphorylated bands of MLKL were still observed in RIPK3 RHIM mutant-expressing iC8KO MEFs after IFN-γ treatment (Fig. 21), suggesting that a small amount of MLKL was still activated, whereas this low level of activated MLKL was not sufficient to induce MLKL oligomerization and subsequent PS exposure and necroptosis. This slight

phosphorylation of MLKL was supposed to be induced by the auto-phosphorylated overexpressed RIPK3 which was driven by kinase domain dimerization (60). These data also imply that IFN-γ-induced PS exposure and necroptosis require considerable amounts of phosphorylated MLKL for the subsequent oligomerization.

4.5 The formation and shedding of PS-exposing bubbles may be significant for maintaining low levels of active MLKL in IFN-γ-treated caspase-8 negative MEFs

In TNF-induced necroptosis, PS-exposing bubbles are released from the plasma membrane by a budding mechanism which is dependent on the ESCRT machinery (30, 53). Interestingly, my study showed that IFN-γ-induced necroptotic cells also released PS-exposing bubbles (Fig. 22). I wonder whether the same mechanism as TNF-induced necroptosis would be involved in the formation and shedding of the PS-exposing bubbles described in this research. Therefore, further studies are needed to elucidate the mechanisms and physiological significance of these findings.

The data of my IFN-γ-induced PS-exposing model indicate that activated MLKL trimer was able to expose PS for more than 10 h without disrupting membrane integrity. During this long PS-exposing period, a low level of MLKL trimer may be necessary for indirectly (or possibly directly) externalizing PS, and the subsequent increased amounts of MLKL trimer may gradually stimulate the membrane rupture to execute necroptosis. Increased MLKL expression induced by IFN-γ seemed to contribute to the conversion of MLKL trimer activity from indirectly (or possibly directly) externalizing PS to disrupting the plasma membrane. In addition, the formation and shedding of IFN-γ-induced PS-exposing bubbles that may contain intracellular MLKL timer, were also considered to maintain the low expression level of MLKL trimer to only induce PS exposure but were not sufficient to induce membrane rupture.

In conclusion, my findings regarding IFN-γ-induced PS exposure and necroptosis have provided insights into the underlying mechanisms and physiological roles of PS

exposure in non-apoptotic cell death. It should be further investigated whether the “eat me” and/or “find me” signals from IFN-γ-induced PS-exposing cells mediate the phagocytosis and/or modulate the inflammatory responses.

References

1. Leventis, P. A. and Grinstein, S. (2010) The distribution and function of phosphatidylserine in cellular membranes. *Annu. Rev. Biophys.* 39, 407-427
2. Kerr, J. F., Wyllie, A. H., and Currie, A. R. (1972) Apoptosis: a basic biological phenomenon with wide-ranging implications in tissue kinetics. *Br. J. Cancer* **26**, 239-257
3. Segawa, K. and Nagata, S. (2015) An Apoptotic 'Eat Me' Signal: Phosphatidylserine Exposure. *Trends Cell Biol.* 25, 639-650
4. Fadok, V. A., Voelker, D. R., Campbell, P. A., Cohen, J. J., Bratton, D. L., and Henson, P. M. (1992) Exposure of phosphatidylserine on the surface of apoptotic lymphocytes triggers specific recognition and removal by macrophages. *J. Immunol.* 148, 2207-2216
5. Segawa, K., Suzuki, J., and Nagata, S. (2014) Flippases and scramblases in the plasma membrane. *Cell Cycle* 13, 2990-2991
6. Suzuki, J., Imanishi, E., and Nagata, S. (2014) Exposure of phosphatidylserine by Xk-related protein family members during apoptosis. *J. Biol. Chem.* 289, 30257-30267
7. Suzuki, J., Denning, D. P., Imanishi, E., Horvitz, H. R., and Nagata, S. (2013) Xk-related protein 8 and CED-8 promote phosphatidylserine exposure in apoptotic cells. *Science* 341, 403-406
8. Hankins, H. M., Baldridge, R. D., Xu, P., and Graham, T. R. (2015) Role of flippases, scramblases and transfer proteins in phosphatidylserine subcellular distribution. *Traffic*16, 35-47
9. Suzuki, J., Umeda, M., Sims, P. J., and Nagata, S. (2010) Calcium-dependent phospholipid scrambling by TMEM16F. *Nature* 468, 834-838
10. Krysko, D. V., Vanden Berghe, T., D'Herde, K., and Vandenabeele, P. (2008) Apoptosis and necrosis: detection, discrimination and phagocytosis. *Methods* 44, 205-221
11. Goldstein, J. C., Kluck, R. M., and Green, D. R. (2000) A single cell analysis of apoptosis. Ordering the apoptotic phenotype. *Ann. N Y Acad. Sci.* 926, 132-141
12. Nagata, S., Hanayama, R., and Kawane, K. (2010) Autoimmunity and the clearance of dead cells. *Cell* 140, 619-630

13. Poon, I. K., Lucas, C. D., Rossi, A. G., and Ravichandran, K. S. (2014) Apoptotic cell clearance: basic biology and therapeutic potential. *Nat. Rev. Immunol.* 14, 166-180

14. Toda, S., Hanayama, R., and Nagata, S. (2012) Two-step engulfment of apoptotic cells. *Mol Cell Biol.* 32, 118-125

15. Miyasaka, K., Hanayama, R., Tanaka, M., and Nagata, S. (2004) Expression of milk fat globule epidermal growth factor 8 in immature dendritic cells for engulfment of apoptotic cells. *Eur. J. Immunol.* 34, 1414-1422

16. Hitomi, J., Christofferson, D. E., Ng, A., Yao, J., Degterev, A., Xavier, R. J., and Yuan, J. (2008) Identification of a molecular signaling network that regulates a cellular necrotic cell death pathway. *Cell* 135, 1311-1323

17. Dondelinger, Y., Hulpiau, P., Saeys, Y., Bertrand, M. J. M., and Vandenabeele, P. (2016) An evolutionary perspective on the necroptotic pathway. *Trends Cell Biol.* 26, 721-732

18. Laster, S. M., Wood, J. G., and Gooding, L. R. (1988) Tumor necrosis factor can induce both apoptic and necrotic forms of cell lysis. *J. Immunol.* 141, 2629-2634.

19. Zhou, Z., Han, V., and Han, J. (2012) New components of the necroptotic pathway. *Protein Cell* 3, 811-817

20. Green, D.R. (2005) Apoptotic pathways: ten minutes to dead. *Cell* 121, 671–67

21. Cho, Y. S., Challa, S., Moquin, D., Genga, R., Ray, T. D., Guildford, M., and Chan, F. K. (2009) Phosphorylation-driven assembly of the RIP1-RIP3 complex regulates programmed necrosis and virus-induced inflammation. *Cell* 137, 1112-1123

22. Vercammen, D., Beyaert, R., Denecker, G., Goossens, V., Van, Loo. G., Declercq, W., Grooten, J., Fiers, W., and Vandenabeele, P. (1988) Inhibition of caspase increases the sensitivity of L929 cells to necrosis mediated by tumor necrosis factor. *J Exp Med.* 187, 1477-1485

23. Oberst, A., Dillon, C. P., Weinlich, R., McCormick, L. L., Fitzgerald, P., Pop, C., Hakem, R., Salvesen, G. S., and Green, D. R. (2011) Catalytic activity of the caspase-8-FLIP (L) complex inhibits RIPK3-dependent necrosis. *Nature* 471, 363-367

24. Tenev, T., Bianchi, K., Darding, M., Broemer, M., Langlais, C., Wallberg, F., Zachariou, A., Lopez, J., MacFarlane, M., Cain, K., and Meier, P. (2011) The Ripoptosome, a signaling

platform that assembles in response to genotoxic stress and loss of IAPs. *Mol. Cell.* 43,432-448

25. Sun, L., Wang, H., Wang, Z., He, S., Chen, S., Liao, D., Wang, L., Yan, J., Liu, W., Lei, X., and Wang, X. (2012) Mixed lineage kinase domain-like protein mediates necrosis signaling downstream of RIP3 kinase. *Cell* 148, 213-227
26. Wang, H., Sun, L., Su, L., Rizo, J., Liu, L., Wang, L. F., Wang, F. S., and Wang, X. (2014) Mixed lineage kinase domain-like protein MLKL causes necrotic membrane disruption upon phosphorylation by RIP3. *Mol. Cell* 54, 133-146
27. Murphy, JM., Czabotar, P. E., Hildebrand, J. M., Lucet, I. S., Zhang, J. G., Alvarez-Diaz, S., Lewis, R., Lalaoui, N., Metcalf, D., Webb, AI., Young, S. N., Varghese, L. N., Tannahill, G. M., Hatchell, E. C., Majewski, I. J., Okamoto, T., Dobson, R. C., Hilton, D. J., Babon, J. J., Nicola, N. A., Strasser, A., Silke, J., and Alexander, W. S. (2013) The pseudokinase MLKL mediates necroptosis via a molecular switch mechanism. *Immunity.* 39, 443-453.
28. Hildebrand, J. M., Tanzer, M. C., Lucet, I. S., Young, S. N., Spall, S. K., Sharma, P., Pierotti, C., Garnier, J. M., Dobson, R. C., Webb, A. I., Tripaydonis, A., Babon, J. J., Mulcair, M. D., Scanlon, M. J., Alexander, W. S., Wilks, A. F., Czabotar, P. E., Lessene, G., Murphy, J. M., and Silke, J. (2014) Activation of the pseudokinase MLKL unleashes the four-helix bundle domain to induce membrane localization and necroptotic cell death. *Proc. Natl. Acad. Sci. U.S.A.* 111, 15072-15077
29. Varfolomeev, E. E., Schuchmann, M., Luria, V., Chiannilkulchai, N., Beckmann, J. S., Mett, I. L., Rebrikov, D., Brodianski, V. M., Kemper, O. C., Kollet, O., Lapidot, T., Soffer, D., Sobe, T., Avraham, K. B., Goncharov, T., Holtmann, H., Lonai, P., and Wallach, D. (1998) Targeted disruption of the mouse Caspase 8 gene ablates cell death induction by the TNF receptors, Fas/Apo1, and DR3 and is lethal prenatally. *Immunity* 9, 267-276
30. Gong, Y. N., Guy, C., Olauson, H., Becker, J. U., Yang, M., Fitzgerald, P., Linkermann, A., and Green, D. R. (2017) ESCRT-III Acts Downstream of MLKL to Regulate Necroptotic Cell Death and Its Consequences. *Cell* 169, 286-300
31. Zargarian, S., Shlomovitz, I., Erlich, Z., Hourizadeh, A., Ofir-Birin, Y., Croker, B. A., Regev-Rudzki, N., Edry-Botzer, L., and Gerlic, M. (2017) Phosphatidylserine

externalization, "necroptotic bodies" release, and phagocytosis during necroptosis. *PLoS Biol.* 15, e2002711

32. Pestka S, Krause C.D., and Walter M.R. (2004) Interferons, interferon-like cytokines, and their receptors. *Immunol Rev* 202, 8–32
33. Stark, G. R., Kerr, I. M., Williams, B. R., Silverman, R. H., and Schreiber, R. D. (1998) How cells respond to interferons. *Annu. Rev. Biochem.* 67, 227-264
34. Borden, E. C., Sen, G. C., Uze, G., Silverman, R, H., Ransohoff, R. M., Foster, G. R., and Stark, G. R. (2007) Interferons at age 50: past, current and future impact on biomedicine. *Nat. Rev. Drug. Discov.* 6, 975-990
35. Cekay, M.J., Roesler, S., Frank, T., Knuth, A. K., Eckhardt, I., and Fulda, S. (2017) Smac mimetics and type II interferon synergistically induce necroptosis in various cancer cell lines. *Cancer Lett.* 410, 228-237
36. Sakamaki, K., Inoue, T., Asano, M., Sudo, K., Kazama, H., Sakagami, J., Sakata, S., Ozaki, M., Nakamura, S., Toyokuni, S., Osumi, N., Iwakura, Y., and Yonehara, S. (2002) *Ex vivo* whole-embryo culture of caspase-8-deficient embryos normalize their aberrant phenotypes in the developing neural tube and heart. *Cell Death Differ*. 9, 1196–1206
37. Takahashi, S., Futatsugi-Yumikura, S., Fukuoka, A., Yoshimoto, T., Nakanishi, K., and Yonehara, S. (2013) Fas deficiency in mice with the Balb/c background induces blepharitis with allergic inflammation and hyper-IgE production in conjunction with severe autoimmune disease. *Int. Immunol.* 25, 287-293
38. Okamoto, K., Fujisawa, J., Reth, M., and Yonehara, S. (2006) Human T-cell leukemia virus type-I oncoprotein Tax inhibits Fas-mediated apoptosis by including cellular FLIP through activation of NF-κB. *Genes Cells* 11, 177-191
39. Hanayama, R., Tanaka, M., Miwa, K., Shinohara, A., Iwamatsu, A., and Nagata, S. (2002) Identification of a factor that links apoptotic cells to phagocytes. *Nature* 417, 182-187
40. Kami, D., Takeda, S., Itakura, Y., Gojo, S., Watanabe, M., and Toyoda, M. (2011) Application of Magnetic Nanoparticles to Gene Delivery. *Int. J. Mol. Sci.* 12, 3705-3722.
41. Thomas, M., Lu, J. J., Ge, Q., Zhang, C., Chen, J., and Klibanov, A. M. (2005) Full deacylation of polyethylenimine dramatically boosts its gene delivery efficiency and

specificity to mouse lung. *Proc. Natl. Acad. Sci.* 102, 5679-5684

42. Mann, J. F., McKay, P. F., Arokiasamy, S., Patel, R. K., Klein, K., and Shattock, R. J. (2013) Pulmonary delivery of DNA vaccine constructs using deacylated PEI elicits immune responses and protects against viral challenge infection. *J. Control Release* 170, 452-459
43. Kobayashi, Y. and Yonehara, S. (2009) Novel cell death by downregulation of eEF1A1 expression in tetraploids. *Cell Death Differ.* 16, 139-150
44. Kiriyama, M., Kobayashi, Y., Saito, M., Ishikawa, F., and Yonehara, S. (2009) Interaction of FLASH with arsenite resistance protein 2 is involved in cell cycle progression at S phase. *Mol. Cell Biol.* 29, 4729-4741
45. Lee, K. K. and Yonehara, S. (2002) Phosphorylation and dimerization regulate nucleocytoplasmic shuttling of mammalian STE20-like kinase (MST). *J. Biol. Chem.* 277, 12351-12358
46. Degterev, A., Huang, Z., Boyce, M., Li, Y., Jagtap, P., Mizushima, N., Cuny, G. D., Mitchison, T. J., Moskowitz, M. A., and Yuan, J. (2005) Chemical inhibitor of nonapoptotic cell death with therapeutic potential for ischemic brain injury. *Nat. Chem. Biol.* 1, 112-119
47. Li, J., McQuade, T., Siemer, A. B., Napetschnig, J., Moriwaki, K., Hsiao, Y. S., Damko, E., Moquin, D., Walz, T., McDermott, A., Chan, F. K., and Wu, H. (2012) The RIP1-RIP3 Necrosome Forms a Functional Amyloid Signaling Complex Required for Programmed Necrosis. *Cell* 150, 339-350.
48. Sun, X., Yin, J., Starovasnik, M. A., Fairbrother, W. J., and Dixit, V. M. (2002) Identification of a novel homotypic interaction motif required for the Phosphorylation of Receptor-interacting Protein (RIP) by RIP3. *J. Biol. Chem.* 277, 9505-9511
49. Zhao, J., Jitkaew, S., Cai, Z., Choksi, S., Li, Q., Luo, J., and Liu, Z. G. (2012) MLKL is a key receptor interacting protein 3 downstream component of TNF-induced necrosis. *Proc. Natl. Acad. Sci.* 109, 5322-5327
50. Chen, X., Li, W., Ren, J., Huang, D., He, W. T., Song, Y., Yang, C., Li, W., Zheng, X., Chen, P., and Han, J. (2014) Translocation of mixed lineage kinase domain-like protein to plasma membrane leads to necrotic cell death. *Cell Res.* 24, 105-121

51. Cai, Z., Jitkaew, S., Zhao, J., Chiang, H. C., Choksi, S., Liu, J., Ward, Y., Wu, L. G., and Liu, Z. G. (2014) Plasma membrane translocation of trimerized MLKL protein is required for TNF-induced necroptosis. *Nat. Cell Biol.* 16, 55-65

52. Liu, S, Liu, H., Johnston, A., Hanna-Addams, S., Reynoso. E., Xiang, Y., and Wang, Z. (2017) MLKL forms disulfide bond-dependent amyloid-like polymers to induce necroptosis. Proc. Natl. Acad. Sci. U.S.A. 114, 7450-7459

53. Yoon, S., Kovalenko, A., Bogdanov, K., and Wallach, D. (2017) MLKL, the Protein that Mediates Necroptosis, Also Regulates Endosomal Trafficking and Extracellular Vesicle Generation. *Immunity* 47, 51-65

54. Tanzer M. C., Khan, N., Rickard, J. A, Etemadi, N., Lalaoui, N., Spall, S. K., Hildebrand, J. M., Segal, D., Miasari, M., Chau, D., Wong, W. L., McKinlay, M., Chunduru, S. K., Benetatos, C. A., Condon, S. M., Vince, J. E., Herold, M. J, and Silke, J. (2017) Combination of IAP antagonist and IFNγ activates novel caspase-10- and RIPK1-dependent cell death pathways. *Cell Death Differ.* 24, 481-491

55. Vermes, I., Haanen, C., Steffens-Nakken, H., and Reutelingsperger, C. (1995) A novel assay for apoptosis. Flow cytometric detection of phosphatidylserine expression on early apoptotic cells using fluorescein labelled Annexin V. *J. Immunol. Methods* 184, 39-51

56. Wang, H., Meng, H., Li, X., Zhu, K., Dong, K., Mookhtiar, A. K., Wei, H., Li, Y., Sun, S. C., and Yuan, J. (2017) PELI1 functions as a dual modulator of necroptosis and apoptosis by regulating ubiquitination of RIPK1 and mRNA levels of c-FLIP. *Proc. Natl. Acad. Sci. U.S.A.* 114, 11944-11949

57. Balachandran, S. and Adams, G. P. (2013) Interferon-γ-induced necrosis: an antitumor biotherapeutic perspective. *J. Interferon Cytokine Res.* 33, 171-18

58. Thapa, R. J., Nogusa, S., Chen, P., Maki, J. L., Lerro, A., Andrake, M., Rall, G. F., Degterev, A., and Balachandran, S. (2013) Interferon-induced RIP1/RIP3-mediated necrosis requires PKR and is licensed by FADD and caspases. *Proc. Natl. Acad. Sci. U.S.A.* 110, E3109-E31188

59. Sun, L., Wang, H., Wang, Z., He, S., Chen, S., Liao, D., Wang, L., Yan, J., Liu, W., Lei, X., and Wang, X. (2012) Mixed lineage kinase domain-like protein mediates necrosis signaling

downstream of RIP3 kinase. *Cell* 148, 213-227

60. Raju, S., Whalen, D. M., Mengistu, M., Swanson, C., Quinn, J. G., Taylor, S. S., Webster, J. D., Newton, K., and Shaw, A. S. (2018) Kinase domain dimerization drives RIPK3-dependent necroptosis. *Sci. Signal.* 11

Abbreviations

BF	bright field
CHO	Chinese hamster ovary
CHX	cycloheximide
C8KO	*Caspase-8* knockout
DMEM	Dulbecco's modified Eagle's medium
DTT	dithiothreitol
EV	empty vector
FACS	fluorescence-activated cell sorting
FADD	Fas-associated death domain protein
FBS	fetal bovine serum
GFP	green fluorescent protein
iC8KO	immortalized C8KO
IAP	inhibitor of apoptosis protein
IFN-γ	interferon gamma
Ig	immunoglobulin
kDa	kilo Dalton
mRNA	messenger RNA
MEF	mouse embryonic fibroblast
MFG-E8	milk fat globule epidermal growth factor 8
MLKL	mixed lineage kinase domain-like protein

Nec-1 (N)	necrostatin-1
NSA	necrosulfonamide
PBS	phosphates-buffered saline
PCR	polymerase chain reaction
pMLKL	phosphorylated MLKL
PI	propidium iodide
PS	phosphatidylserine
PVDF	polyvinylidene fluoride
qRT-PCR	quantitative reverse transcription PCR
RIPK1	receptor-interacting protein kinase 1
RIPK3	receptor-interacting protein kinase 3
RHIM	RIP homotypic interaction motif
SDS	sodium dodecyl sulfate
SDS-PAGE	SDS-polyacrylamide gel electrophoresis
shRNA	short hairpin RNA
STS	staurosporine
TMEM16F	transmembrane protein 16F
TNF	tumor necrosis factor
TRAIL	TNF-related apoptosis-inducing ligand
UV	ultraviolet
WT	wild-type

Acknowledgements

First and foremost, I would like to deeply thank Prof. Shin Yonehara for his enormous support and helpful advice and comments during the study of my doctoral course, for his wide expertise in the field of molecular biology in apoptotic and necroptotic cell death, and for always being open-eared to listen to my opinions when I met troubles in studies or daily life. Under the guidance of him, I successfully finished my research.

I am also grateful to all the members (including old boys and old girls) of Yonehara Laboratory. I especially thank Hirotaka Kazama Ph.D. and Akira Murakami Ph.D.; they taught me how to learn from scratch in the field of molecular biology, and I learned a lot of experimental techniques from them.

I address my thanks to Prof. Shigekazu Nagata for providing cDNA of mouse MFG-E8 (D89E), TMEM16F KO MEFs, and anti-mouse TMEM16F antibody, and to Prof. Tatsushi Igaki to be the chief examiner of my doctoral dissertation, thank you!

Finally, I dedicate my warmest thanks to my parents, for giving me the biggest support and encouragement during these years in Japan.

This doctoral thesis is written based on the content of the academic paper shown below.

Jiancheng Chen, Shunsuke Kuroki, Masataka Someda, and Shin Yonehara

Interferon-γ induces the cell surface exposure of phosphatidylserine by activating the protein MLKL in the absence of caspase-8 activity

Journal of Biological Chemistry, in press, 2019